Semiconductor superlattices

A. P. Silin

P. N. Lebedev Physics Institute, Academy of Sciences of the USSR
Usp. Fiz. Nauk **147**, 485–521 (November 1985)

The properties of semiconductor superlattices—solid-state structures in which there exists, in addition to the periodic potential of the crystal lattice, a one-dimensional potential whose period is much longer than the lattice constant—are studied. The existence of the superlattice potential substantially alters the energy spectrum, as a result of which superlattices have a number of interesting properties which ordinary semiconductors do not have. Superlattices offer a unique possibility for altering their band structure practically arbitrarily. The characteristic features of the luminescence of superlattices (tunability of the emitted wavelengths, the excitonic nature of the radiation up to room temperature, strong suppression of impurity trapping, femtosecond kinetics, etc.) are being exploited to develop a new generation of light-emitting devices. The acoustic properties of superlattices are characterized by the existence of selective reflection of phonons. Semiconductor superlattices are characterized by substantially nonlinear transport properties, owing to the presence of very narrow minibands in their energy spectrum.

CONTENTS

1. Introduction ... 972
2. Energy structure ... 973
   2.1. Compositional superlattices. 2.2. Doped superlattices. 2.3. Collective excitations.
3. Optical properties ... 981
   3.1. Intraband processes. 3.2. Interband transitions. Compositional superlattices. 3.3. Interband transitions. Doped superlattices.
4. Acoustical properties ... 985
5. Transport phenomena ... 986
   5.1. Conductivity. 5.2. Shubnikov–de Haas effect.
6. The semimetal-semiconductor transition ... 988
7. Conclusions ... 990
References ... 990

1. INTRODUCTION

Solid state structures which have, in addition to the periodic potential of the crystal lattice, a one-dimensional periodic potential whose period is much longer than the lattice constant are customarily called superlattices.

Superlattices are a new type of semiconductor which is characterized by the presence of a large number of bands, exhibiting very strong anisotropy (they are practically two-dimensional). Such systems were first studied by L. V. Keldysh in 1962.[1] Electron-hole recombination can be almost completely suppressed in superlattices, so that a large departure from thermal equilibrium can exist for long periods of time. The electron and hole densities in superlattices are not fixed parameters determined by the doping, but rather are easily adjustable parameters. The existence of the superlattice potential substantially changes the energy spectrum, as a result of which superlattices have a number of interesting properties which ordinary semiconductors do not. The parameters of the superlattice potential can be easily varied over a wide range, which in its turn gives rise to substantial changes in the energy spectrum. The band structure of semiconductor superlattices can thus be easily altered.

The rapid growth in both theoretical and experimental interest in superlattices is linked to the latest progress in the technology of molecular-beam epitaxy in an ultrahigh vacuum[2,3] (see also the reviews of Refs. 4–8) and metal-organic epitaxy from the gas phase[9] as well as other methods.[10,11]

With the help of these methods it is possible to obtain atomically smooth surfaces and very sharp interfaces. This has enabled controlled growth of high-quality superlattices. The growth rate, for example, constitutes $\sim$Å/sec for GaAs–$Al_xGa_{1-x}As$[12] and InAs-GaSb[4] superlattices grown by the method of molecular-beam epitaxy.

Quantum size effects become significant when one of the dimensions of the semiconductor is decreased to such an extent that it becomes of the order of the electron wavelength. Semiconductor devices can usually be regarded as semiclassical, because their characteristic sizes usually exceed the electron mean free path. If, however, their dimensions are decreased to hundreds of angstroms, then the quantum size effects have a substantial effect on the electronic structure, which is manifested especially vividly in optical and transport phenomena.

Compositional superlattices, which consist of epitaxially grown periodically alternating thin layers of semiconductors with close lattice constants, have been studied in great-

0038-5670/85/110972-22$01.80
© 1986 American Institute of Physics

est detail both theoretically and experimentally.[13] Doped superlattices, whose periodic potential is formed by the alternation of ultrathin n- and p-type layers of the same semiconductor, which can be separated from one another by undoped layers, have also been widely used.[5,6,12] In this review we shall study the properties of these superlattices only.

Two-dimensional superlattices, which are formed when the plane of the surface charge in a two-dimensional electron layer (for example, in a metal-insulator-semiconductor structure) is periodically modulated, are also possible.[14] A surface with high crystalline indices—orientational superlattices—can also be used as superlattices for a two-dimensional electron gas.[15]

Spin superlattices,[16] formed by the periodic repetition of layers of the same semiconductor, are also of interest. Some layers in these superlattices are doped with nonmagnetic impurities, while the others are doped with magnetic impurities; in addition, in the absence of a magnetic field the energy gap is the same in the entire superlattice, while in the presence of a magnetic field a periodic superlattice potential appears. Such superlattices were recently synthesized based on $CdTe$-$Cd_{1-x}Mn_xTe$.[17]

A superlattice potential can also be created by a periodic deformation of the sample in the field of an intense ultrasonic wave[1] or a standing light wave.[18] Dichalcogenides of transition metals, group A_3B_6 semiconductors, polytypic semiconducting compounds, and others[19] can be regarded as natural superlattices.[19]

Deviations from periodicity during the preparation of superlattices can destroy the character of the spectrum, i.e., current carriers can become trapped in one of the minima of the superlattice potential. In addition, the scattering of current carriers creates an uncertainty $\sim\hbar/\tau$ (τ is the characteristic relaxation time) in their energy. If τ is quite short, then the spectrum created by the superlattice potential will not be distinguishable. In order for this not to happen, the mean free path of the current carriers l must be much longer than the period of the superlattice d [19]:

$$l \gg d. \qquad (1.1)$$

In this review we shall study the so-called isolated quantum wells, a typical example of which is the double heterojunction (Fig. 1). A number of the physical properties of isolated quantum wells (optical properties, transport properties in the plane of the layers) are in many ways analogous to the properties of semiconductor superlattices with a large quantum barrier thickness d_{II} (Fig. 2) (the so-called system of multiply repeating quantum wells[6]).

The early (up to 1974), primarily theoretical, literature on superlattices is discussed in detail in Ref. 19. The properties of $In_{1-x}Ga_xAs$-$GaSb_{1-y}As_y$ compositional superlattices are reviewed in Ref. 4; the reviews of Refs. 5, 6, and 12 are devoted primarily to doped superlattices.

A quite complete list of references devoted to semiconductor superlattices consisting of A_3B_5 compounds and published in 1958–1983 is given in Ref. 20.

Historically the prediction of a number of anomalies in the transport properties of semiconductor superlattices, in particular, negative differential conductivity, and the possibility of their exploitation for practical applications[13] led to the creation of the first superlattices.[21,22] Later, however, the substantial progress achieved in the study of the optical properties of semiconductor superlattices diverted the attention of experimenters away from the study of the transport properties of superlattices.[8] In this review we shall study primarily the energy structure (Sec. 2) and optical properties (Sec. 3) of semiconductor superlattices, which have thus far been studied in greatest detail (especially experimentally), and we shall discuss only briefly the acoustic (Sec. 4) and transport (Sec. 5) properties, as well as the semimetal-semiconductor transition in superlattices (Sec. 6).

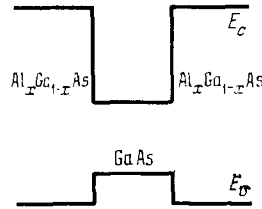

FIG. 1. Energy structure of the double heterojunction $Al_xGa_{1-x}As$-$GaAs$-$Al_xGa_{1-x}As$.

2. ENERGY STRUCTURE

The physical properties of superlattices are determined by their electronic spectrum, which in its turn is determined by the solution of Schrödinger's equation contain both the crystal-lattice potential and the superlattice potential $\Delta(\mathbf{r})$. It is virtually impossible to solve this equation in the general case. The problem simplifies substantially, however, because of the fact that the period of the superlattice is much longer than the lattice constant, and the amplitude of the superlattice potential is much smaller than the amplitude of the crystalline superlattice. Because of this the energy bands of semiconductors existing before $\Delta(\mathbf{r})$ is superposed will be distorted by it only near the edges. Superlattices consisting of metals are therefore of little interest (since the Fermi level in metals lies far from the band edges).[19] In this review we shall confine our attention to semiconductor superlattices only; we shall ignore metal[23] and superconductor[24] superlattices.

Because the superlattice potential distorts the energy bands of semiconductors near the edges only, the dispersion law of the current carriers may be assumed to be quadratic and the energy structure of superlattices can be found in the

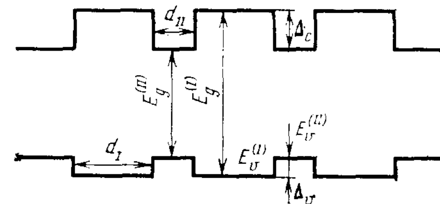

FIG. 2. Energy structure of type I compositional superlattices. I) GaAs semiconductor; II) $Al_xGa_{1-x}As$.

effective mass approximation, which in the simplest one-band approximation for nondegenerate isotropic energy bands has the following form

$$-\frac{\hbar^2}{2m_{c(v)}}\nabla^2\psi(\mathbf{r})+\Delta_{c(v)}(\mathbf{r})\psi(\mathbf{r})=E\psi(\mathbf{r}), \qquad (2.1)$$

where $m_{c(v)}$ is the effective mass of an electron (hole), which here we shall assume to be the same throughout the entire superlattice.

Depending on the nature of the periodicity of $\Delta(\mathbf{r})$, superlattices can be 1-, 2-, and 3-dimensional. In this review we shall study only one-dimensional superlattices $\Delta(z)$. A quasi-two-dimensional variant of superlattices, based on size-quantized layers of $Al_xGa_{1-x}As$ with an energy miniband limited in two directions and with a fixed energy in the direction perpendicular to the layers (see, for example, Refs. 25–27), is also possible:

$$E(k)=2\Delta-\Delta(\cos k_xd+\cos k_yd), \qquad (2.2)$$

where Δ is the width of the miniband.

Since the superlattice potential $\Delta_{c(v)}(z)$ is periodic, the wave function $\psi(z)$ has the Bloch form, while the spectrum has a band character and is determined by the band number j and wave vector k_z. The bands (minibands) so obtained represent a finer division of the energy bands near their edges. The wave vector k_z is determined in the first Brillouin miniband $-\pi/d\leqslant k_z\leqslant\pi/d$. The complete wave function of the current carriers in the superlattice is given by the product of the envelop function $\psi(z)$ and the modulating Bloch function at the point of the band extremum.

The energy spectrum of one-dimensional superlattices is markedly anisotropic. While the superlattice potential has little effect on the motion of the current carriers perpendicular to the axis of the superlattice z, motion in the z direction will correspond to the motion in a system with a period d:

$$E(\mathbf{k})=\frac{\hbar^2\mathbf{k}_\perp^2}{2m}+E_j(k_z), \qquad (2.3)$$

so that $|k_z|\leqslant\pi/d$. For fixed $\mathbf{k}_\perp$ the dispersion curve of a bulk semiconductor $E(k_z)$ separates into Brillouin minibands $E_j(k_z)$, separated by minigaps at $k_z=0$ and $k_z=\pm\pi/d$ (Fig. 3).

The qualitative features of the energy structure of semiconductor superlattices are the same for different superlattices (different $\Delta(z)$). The spectrum $E_j(k_z)$ consists of a series of nonoverlapping minibands. As the miniband number j increases, the width of the miniband increases while the width of the energy minigap decreases. If the energy of the miniband is less than the maximum of the superlattice potential, then such minibands have a small width, determined by the tunneling transparency of the barriers in the superlattice, and can be described in the strong coupling approximation (see, for example, Ref. 19):

$$E_j(k_z)=E_j-\Delta_j\cos k_zd; \qquad (2.4)$$

where E_j are the energy levels of an individual well and $|\Delta_j|$ is the width of the jth miniband, which is determined by the superlattice parameters.

Minibands with energies lying above the maximum of the superlattice potential consist of wide sections with the usual quadratic spectrum, separated by narrow minigaps whose width corresponds to the Fourier harmonic of $\Delta(z)$.[19]

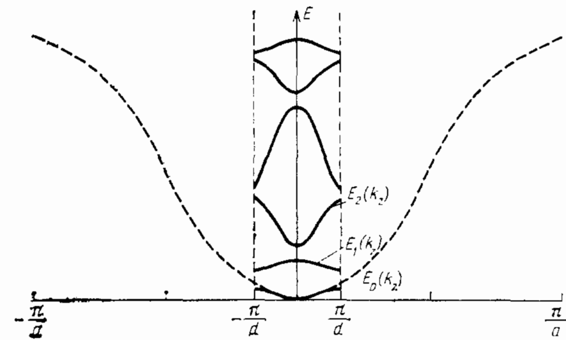

FIG. 3. Splitting of the energy band $E(k_z)$ of a crystal with a lattice constant a into minibands $E_j(k_z)$ by the superlattice potential with period d. The number of minibands is equal to d/a.

The positions and widths of the energy minibands of semiconductor superlattices can be evaluated for a superlattice potential of an arbitrary form $\Delta(z)\neq E$ from general considerations[28]

$$[(E_{2j-1}-E_0)^{1/2}-(E_{2(j-1)}-E_0)^{1/2}]^2<\frac{\hbar^2\pi^2}{2md^2}, \qquad (2.5)$$

where the energy intervals $(E_{2(j-1)}, E_{2j-1})$ correspond to allowed bands ($j=1, 2,\ldots$).

2.1. Compositional superlattices

We shall study the energy structure of compositional superlattices—superlattices consisting of ultrathin ($\sim 10^1$–10^3 Å) layers of different semiconductors. To obtain good compositional superlattices it is important that the lattice constants of the constituent semiconductors of the superlattice be close to one another.

There are three types of compositional superlattices: 1) superlattices ($GaAs$–$Al_xGa_{1-x}As$), in which the minimum of the conduction band ($E_c^{(I)}$) and the maximum of the valence band ($E_v^{(I)}$) of one semiconductor ($GaAs$) lie inside the energy gap of the other semiconductor ($Al_xGa_{1-x}As$) (see Fig. 2); 2) superlattices ($InAs$-$GaSb$), in which the minimum of the conduction band ($E_c^{(I)}$) of one semiconductor ($InAs$) lies below the maximum of the valence band ($E_v^{(II)}$) of the other semiconductor ($GaSb$) (Fig. 4); 3) the superlattices ($In_xGa_{1-x}As$-$GaSb_{1-y}As_y$ with $x\approx y\approx 1-x$), in which the minimum of the conduction band ($E_c^{(I)}$) of one semiconductor ($In_xGa_{1-x}As$) lies in the energy gap

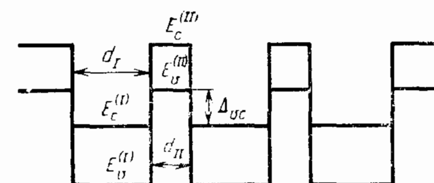

FIG. 4. Energy structure of a type III compositional superlattice. I) InAs; II) GaSb.

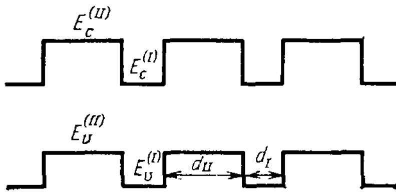

FIG. 5. Energy structure of a type III compositional superlattice. I) the semiconductor $In_xGa_{1-x}As$; II) $GaSb_{1-y}As_y$.

($E_g^{(II)}$) of the second semiconductor ($GaSb_{1-y}As_y$), while the maximum of the valence band of the second semiconductor ($E_v^{(II)}$) lies in the energy gap of the first semiconductor ($E_g^{(I)}$) (Fig. 5).

In type I compositional superlattices (see Fig. 2) layers of two semiconductors with thicknesses d_I and d_{II} and energy gaps $E_g^{(I)}$ and $E_g^{(II)}$ alternate, giving rise to a periodic system of quantum wells for current carriers (first semiconductor) which are separated from one another by quantum barriers (second semiconductor). The depth of the quantum wells for electrons (holes) is determined by the difference between the minima of the conduction bands $\Delta_c = E_c^{(II)} - E_c^{(I)}$ (maxima of the valence band $\Delta_v = E_v^{(I)} - E_v^{(II)}$) of the two semiconductors. The magnitude of the superlattice potential Δ is defined in this case as the difference of the energy gaps of the two semiconductors:

$$\Delta = E_g^{(II)} - E_g^{(I)} = \Delta_c + \Delta_v; \qquad (2.6)$$

for the superlattices $GaAs-Al_{0.3}As_{0.7}As$, $\Delta = 300$ meV and $\Delta_c = 0.85\Delta_v$.[4]

The motion of electrons parallel to the axis of the superlattice z is quantized. This gives rise to the formation of a series of discrete (for a separate well) energy levels $E_{c,j}$. A rough estimate of $E_{c,j}$ for $E_{c,j} \ll \Delta_c$ gives

$$E_{c,j}(d_I) \approx \frac{\hbar^2\pi^2}{2m_c^{(I)}d_I^2}(j+1)^2, \quad j = 0,\ 1,\ 2,\ \ldots; \qquad (2.7)$$

where $m_c^{(I)}$ is the electron mass in the first semiconductor (GaAs); for $d_I = 100$ Å, $E_{c,0} \approx 50$ meV.

The exact values of $E_{c,j}(k_z)$ can be obtained (if the small difference in the electron effective masses in GaAs and $Al_xGa_{1-x}As$ is ignored) from the solution of Eq. (2.1):

$$\frac{k_{II}^2 - k_I^2}{2k_Ik_{II}} \operatorname{sh} k_{II}d_{II} \cdot \sin k_Id_I + \operatorname{ch} k_{II}d_{II} \cdot \cos k_Id_I = \cos k_zd, \qquad (2.8)$$

where

$$k_{II} = \frac{1}{\hbar}[2m_c^{(I)}(\Delta_c - E_{c,j})]^{1/2}, \quad k_I = \frac{1}{\hbar}(2m_c^{(II)}E_{c,j})^{1/2}. \qquad (2.9)$$

The dispersion of the energy minibands in the strong-coupling approximation has the following form:

$$E_{c,j}(k_z) = E_{c,j} - \Delta_j(d_{II}) \cos k_zd, \qquad (2.10)$$

where $|\Delta_j(d_{II})|$—the width of the jth miniband—depends strongly on the barrier width d_{II}. If the width of the barriers is small, $d_{II} \lesssim 50$ Å, then the minibands have an appreciable width for motion along the axis of the superlattice. Thus, for $d_{II} = 50$ Å $\Delta_{c,0} \approx 10$ meV[6] (Fig. 6).

Thus the required position of the miniband $E_{c,j}$ can be selected by varying the width of the well d_I, and the width of the miniband $|\Delta_{c,j}|$ can be chosen by setting the width of the barrier d_{II}.

The calculation of the valence minibands in compositional superlattices is similar, but it is complicated somewhat by mixing of the light- and heavy-hole states. A more accurate approach must be used in order to take into account the coupling of the valence bands, the nonparabolicity of the energy bands, and the difference in the effective masses of the current carriers in the constituent semiconductors of the superlattice.[29-33] If the constituent semiconductors of the superlattice have the same crystalline structure, lattice constants, and Bloch functions, then the envelope wave functions $\psi(z)$ satisfy the following boundary conditions at the interfaces: 1) $\psi(z)$ and 2) $\left(\frac{1}{\mu(E,z)}\right)\frac{\partial\psi(z)}{\partial z}$ are continuous. Here $\mu(E,z)$ is a quantity with the dimensions of mass, which depends on the energy, if the band structure of the constituent semiconductors of the superlattice is nonparabolic. In group A_3B_5 and A_2B_6 semiconductors (of which the superlattices primarily consist) the band structure is described well by Kane's two-band model.[34] For $k_\perp = 0$ a splitting appears between the heavy-hole band and the light-hole and electron bands and holes from the valence band, split off by the spin-orbital interaction. Taking into account the interaction of the three last bands, the equation in the effective mass approximation has the following form[31-33]:

$$\left[-\frac{\hbar^2}{2}\frac{\partial}{\partial z}\frac{1}{\mu(E,z)}\frac{\partial}{\partial z} + \Delta_c(z)\right]\psi_c(z) = E\psi_0(z), \qquad (2.11)$$

and

$$\frac{1}{\mu(E,z)} = \frac{2P}{3}\left(\frac{2}{E + E_g^{(I)} - \Delta_v(z)} + \frac{1}{E + E_g^{(I)} + E_{s-0}^{1} - \Delta_{s-0}(z)}\right); \qquad (2.12)$$

where ($E_{c-0}^{(I)}$) is the spin-orbital splitting of the first semiconductor; $\Delta_c(z)$, $\Delta_v(z)$, $\Delta_{s-0}(z)$ are functions which vanish in the first semiconductor while Δ_c, Δ_v, Δ_{s-0} vanish in the second semiconductor (Δ_{s-0} is the difference between the maxima of the valence band split by spin-orbital interaction); and, P is the Kane matrix element.[34] For wide-gap semiconductors ($E \ll E_g^{(I)}, |E - \Delta_c| \ll E_g^{(II)}$)

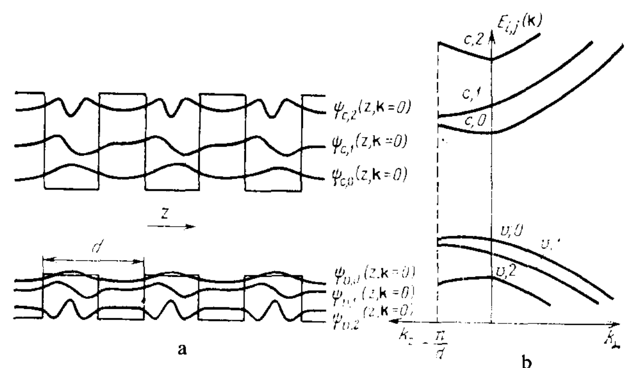

FIG. 6. Electronic structure of a type I compositional superlattice: in coordinate space (a) and in momentum space (b).

$$\mu(E, z) = \begin{cases} m_c^{(I)} & \text{in the first semiconductor,} \\ m_c^{(II)} & \text{in the second semiconductor.} \end{cases} \quad (2.13)$$

This method was used to calculate the type I superlattice of GaAs-$Al_xGa_{1-x}As$,[31] HgTe-CdTe,[32,35] and many others.

The energy structure of the type I compositional superlattices GaAs-$GaAs_{1-x}P_x$ and GaAs-$Al_xGa_{1-x}As$ was calculated in Ref. 29, taking into account the nonparabolicity of the band structure of the constituent semiconductors of the superlattice.

The compositional superlattice GaAs-AlAs was calculated with the help of the pseudopotential method in Ref. 36, where the band structure of this superlattice and that of the alloy $Al_{0.5}Ga_{0.5}As$ was also compared.

A calculation of the band structure of the type I compositional superlattice Si-GaP showed that in superlattices with the composition A_4-A_3B_5, unlike superlattices with the composition A_3B_5-$A_3'B_5'$, characteristic states can appear at the interfaces.[37]

In type I compositional superlattices there are no current carriers in the ground state, so that doping of these superlattices is of special interest.[38] The binding energy of an isolated donor (Si) in bulk GaAs is equal to 6 meV, while in bulk $Al_{0.3}Ga_{0.7}As$ it is $\gtrsim 100$ meV. Because of the fact that the minimum of the conduction band of GaAs lies below the donor state in $Al_{0.3}Ga_{0.7}As$, electrons from the donor centers $Al_{0.3}Ga_{0.7}As$ flow into the conduction band in GaAs, thereby creating depleted layers of $Al_{0.3}Ga_{0.7}As$. This gives rise to curving of the energy bands of the constituent semiconductors of the superlattice (Fig. 7).

Modulation-doped type I compositional superlattices (Fig. 7b), differing from uniformly doped superlattices (Fig. 7a) by the fact that only the $Al_xGa_{1-x}As$ layers are doped, have interesting properties. Here the mobile current carriers (electrons) lie in the GaAs layers, and their donor impurity centers lie in $Al_xGa_{1-x}As$. It is thus possible to create a high current-carrier density in GaAs, much higher than the density of the impurity scattering centers present in GaAs. This substantially increases the mobility of electrons in the temperature range where impurity scattering is determining. The mobility increases especially significantly if the barrier regions near the interfaces are not doped.[39] For impurity concentrations exceeding 10^{16} cm^{-3}, the current carriers are not frozen out[18] and electron densities exceeding 10^{12} cm^{-2} and mobilities higher than 10^6 cm^2/V sec can be achieved in modulation-doped superlattices.[40]

In type II compositional superlattices (see Fig. 4) the top of the valence band of one semiconductor (GaSb) lies above the bottom of the conduction band of the other semiconductor (InAs); it may thus be expected that electrons will flow through the interface from the valence band of GaSb into the conduction band of InAs. The semimetallic state so formed is characterized by strong interaction of the two-dimensional electron and hole gases. If the thickness of the superlattice layers is quite small, however, then the size quantization of the motion of the current carriers (2.7) can change the mutual positions of the conduction band in InAs and the valence band in GaSb (a type III compositional superlattice forms (Fig. 5)). The semimetal-semiconductor transition, which occurs in such superlattices when the superlattice period is decreased, has been observed experimentally (this is discussed in greater detail in Sec. 6).

The band structure of type II and III compositional superlattices is calculated in Refs. 30–32 and 41–49.

The type II compositional superlattices AnAs-AlSb-GaSb,[50] in which the InAs and GaSb layers are separated by AlSb layers, whose energy gap is much larger than that of InAs and GaSb, have also been created. Tunneling of electrons from GaSb into InAs through the AlSb layers will also occur in such superlattices. The band structure of such superlattices was calculated in Ref. 32.

In calculating the band structure of type II compositional superlattices the following must be taken into account. 1) The small magnitude of the energy gaps of the constituent semiconductors of the superlattice and the strong mixing of the states of the valence band of one semiconductor (GaSb) and of the states of the conduction band of the other (InAs) occurring at the interfaces necessitate a multiband analysis of these superlattices. 2) An adequate description of the extrema of the energy bands, especially of the degenerate valence band, is necessary in order to study the dynamics of current carriers with momenta perpendicular to the axis of the superlattice. (It should be noted, however, that a small (0.62%) mismatch of the lattice constants in InAs and GaSb gives rise to splitting of the valence band of GaSb; thus, if the InAs layer is 120 Å thick and the GaSb layer is 80 Å thick, then this splitting is equal to 26 meV.[51]) 3) The existence of a flow of current carriers through the interface requires a self-consistent calculation of the band structure.[46,47] 4) The formation of a high-density quasi-two-dimensional system of electrons and holes as a result of the flow of current carriers makes it necessary to take into account many-body effects.[52–53]

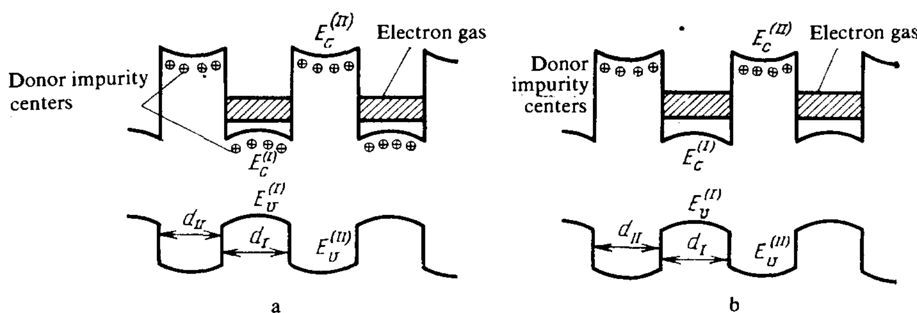

FIG. 7. The energy structure of type I compositional superlattices. I) the semiconductor GaAs; II) $AlGa_{1-x}As$; a) uniformly doped superlattice, b) modulation-doped superlattice.

The large size of the unit cell, on the other hand, makes it difficult to carry out a complete microscopic calculation.

A calculation of the energy-band structure taking into account the requirements 1) and 2) was carried out in Refs. 46, 47, and 49.

Until recently the epitaxy of heterostructures (including also of compositional superlattices) was limited to semiconductors with equal lattice constants a. A small but finite mismatch of the lattice constants δa is accompanied by both elastic deformations and the formation of a high density of defects $n_d \sim 2\delta a/a^3$.[51] Compositional superlattices with a large mismatch of the lattice constants $\delta a/a \sim 1\%$ (the so-called stressed superlattices), in which misfit dislocations are absent, have recently been successfully grown. This is attributable to the fact that if the layers of the stressed superlattices are quite thin ($\lesssim 100$ Å), then they deform elastically and the density of defects at the interfaces remains low[54]; this is confirmed by the high level of stimulated emission as well as by examination under an electron microscope.[55]

Growing stressed superlattices makes it possible to expand substantially the class of semiconducting compounds which are suitable for creating compositional superlattices. The stressed superlattices GaP-$GaAs_xP_{1-x}$[56,57] and GaAs-$In_{1-x}Ga_xAs$,[58–60] in which the ternary compound has the smaller gap, as well as GaSb-AlSb[61,62] are of special interest.

A study of the absorption[63] and emission[64–65] of light in the stressed superlattice GaSb-AlSb showed that this is a type I compositional superlattice[63] and made it possible to determine the decrease in the energy gap of GaSb caused by elastic deformations. The lattice constants are equal to $a_I = 6.0955$ Å (GaSb), $a_{II} = 6.1355$ Å (AlSb). In the superlattice the GaSb layers are stretched and the AlSb layers are compressed in directions perpendicular to the axis of the superlattice.[51]

The superlattices GaAs-$In_xGa_{1-x}As$,[58–60] in which $In_xGa_{1-x}As$ are compressed and GaAs are stretched, are type I superlattices for small x and type III superlattices for large x.[51]

In the type II superlattices InAs-GaSb the splitting of the valence band[51] caused by the mismatch of the lattice constants can explain the disagreement between the theoretical[46–49] and experimenal[4,66–69] results.

The stressed type I superlattices ZnS-ZnSe with a large mismatch of the lattice constants ($\delta a/a \sim 5\%$) were recently synthesized.[69]

An analysis of the band structure of stressed superlattices taking into account the deformations appearing in them (in particular, the change in the relative energies of the light- and heavy-hole minibands) is presented in Ref. 51.

The compositional superlattices $Al_xGa_{1-x}As$, in which x varies linearly from zero at the beginning of a period up to 0.2 at the end of the period (the period is equal to 500 Å)[70] (Fig. 8) have also been grown. These saw-tooth-shaped superlattices are characterized by periodic alternation of triangular wells and barriers and exhibit interesting transient polarization phenomena (see Sec. 3.2). The band structure of these superlattices is calculated in Ref. 71.

Amorphous superlattices are an interesting class of compositional superlattices. Superlattices consisting of amorphous hydrogenated semiconductors (a-Si: H, a-$Si_{1-x}N_x$: H, a-Ge: H, a-$Ge_{1-x}N_x$: H) have been synthesized. In these semiconductors the lattice constants do not match and the layers are not epitaxial. The requirement that the lattice constants match is, however, eased for amorphous semiconductors.

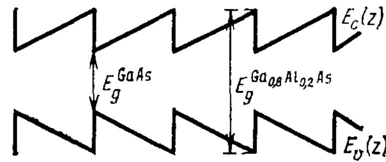

FIG. 8. Energy structure of the saw-tooth superlattice $Ga_{1-x}Al_xAs$.

The interfaces of these superlattices do not have defects and are atomically smooth.[72,73] The amorphous superlattices $As_{40}Se_{60}$-$Ge_{25}Se_{75}$ have also been grown.[74]

We call attention to compositional superlattices in which the barrier layers (GaAs, Ge, Si) are not oriented, while the quantum-well layers (InSb, PbTe, and CdTe) are single-crystalline.[75]

Compositional superlattices in which the effective potential is created not by a periodic change in the position of the energy bands, but rather by a change in the effective masses are also possible.[76]

2.2. Doped superlattices

The substantial improvement in the spatial (on an atomic scale) monitoring of the doping during film growth by means of molecular-beam epitaxy enabled growing doped superlattices—periodic alternation of thin (~ 10–10^3 Å) layers of GaAs of the n (GaAs: Si)- and p(GaAs: Be)-types, separated in many cases by layers of intrinsic GaAs (the so-called nipi crystals (Fig. 9)). Many of the electronic properties of doped superlattices were predicted theoretically.[77]

The superlattice potential in doped superlattices is created solely by the spatial distribution of the charge. From the crystallographic viewpoint these superlattices have some advantages over compositional superlattices. The introduction of impurities (there are always many fewer impurity atoms than atoms of the main semiconductor) has virtually no effect on the lattice of the main crystal. The problems associated with the presence of interfaces therefore do not arise; also, there are no restrictions on the choice of the main semiconductor.

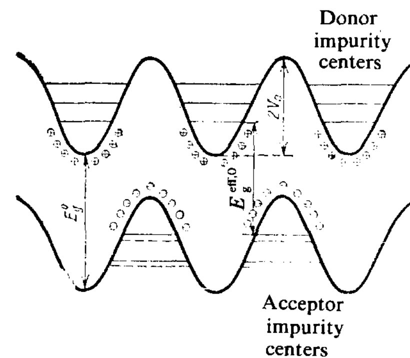

FIG. 9. Energy structure of a doped superlattice.

All donor centers in doped superlattices are positively charged, while all acceptor centers are negatively charged, if the impurity concentration is not too high, while the number of acceptors in the p layers is equal to the number of donors in the n layers.

The contribution of ionized impurities to the superlattice potential is determined by the solution of Poisson's equation[6,78]

$$\frac{d^2V_i(z)}{dz^2}=\frac{4\pi e^2}{\varkappa_0}[n_D(z)-n_A(z)] \qquad (2.14)$$

with the boundary conditions ($z=0$ corresponds to the center of the n layer)

$$\left.\frac{dV_i}{dz}\right|_{z=0}=V_i(0)=0; \qquad (2.15)$$

where $n_{D(A)}(z)$ is the distribution function of the donors (acceptors) and $\varkappa_0$ is the static dielectric permittivity.

If the doping is uniform, then the potential $V_i(z)$ is quadratic in the doped regions (see Fig. 9):

$$V_i(z)=\begin{cases}\frac{2\pi e^2 n_D}{\varkappa_0}z^2, & |z|\leqslant\frac{d_n}{2},\\ 2V_0-\frac{2\pi e^2 n_A}{\varkappa_0}\left(\frac{d}{2}-|z|\right)^2, & \frac{d}{2}-|z|\leqslant\frac{d_p}{2},\end{cases} \qquad (2.16)$$

and linear in the intrinsic regions:

$$V_i(z)=\frac{2\pi e^2 n_D d_n}{\varkappa_0}\left(|z|-\frac{d_n}{4}\right),\quad \frac{d_n}{2}\leqslant|z|\leqslant\frac{d-d_p}{2}; \qquad (2.17)$$

here V_0 is the amplitude of $V_i(z)$:

$$V_0=\frac{\pi e^2}{\varkappa_0}\left(\frac{n_D d_n^2}{4}+\frac{n_A d_p^2}{4}+n_D d_n d_i\right), \qquad (2.18)$$

where $d_{n(p,i)}$ is the width of the n (p,i) layers.[78]

The mobile current carriers (electrons: $n(z)$; holes: $p(z)$) give the Hartree contribution

$$V_H(z)=\frac{4\pi e^2}{\varkappa_0}\int_0^z dz'\int_0^{z'}dz''[-n(z'')+p(z'')] \qquad (2.19)$$

and the exchange-correlation contribution $V_{xc}(z)$ to the superlattice potential.[78]

The distributions $n(z)$ and $p(z)$ are calculated by the energy-functional method,[78] in which the single-particle Schrödinger equation is solved in a self-consistent manner:

$$\left[-\frac{\hbar^2}{2m_i}\nabla^2+V_{cc}(z)\right]\varphi_{i,j,k}(\mathbf{r})=E_{i,j}(\mathbf{k})\varphi_{i,j,k}(\mathbf{r}),$$

$$j=0,1,\ldots, \qquad (2.20)$$

where

$$V_{sc}(z)=V_i(z)+V_H(z)+V_{xc}(z). \qquad (2.21)$$

The index i corresponds to electrons ($i=c$), light holes ($i=lh$), and heavy holes ($i=hh$).

If the mixing of different bands by the potential $V_{cc}(z)$ is neglected, then

$$\varphi_{i,j,k}(r)=e^{i\mathbf{k}_\perp\boldsymbol{\rho}}u_i(\mathbf{r})\psi_{i,j,k_z}(z), \qquad (2.22)$$

where $u_i(r)$ is the Bloch function of the ith band, $\psi_{i,j,k_z}(z)$ is the envelope function of the jth miniband of the ith band, $\boldsymbol{\rho}=(x,y)$, and

$$\left[-\frac{\hbar^2}{2m_i}\frac{d^2}{dz^2}+V_{sc}(z)\right]\psi_{i,j,k_z}(z)=E_{i,j}(k_z)\psi_{i,j,k_z}(z), \qquad (2.23)$$

$$E_{i,j}(\mathbf{k})=\frac{\hbar^2k_\perp^2}{2m_i}+E_{i,j}(k_z). \qquad (2.24)$$

In most cases,[6] the interaction between the neighboring quantum wells can be neglected, i.e., the dependence of the energy on k_z can be neglected. Then the envelope function will have the following form[6]:

$$\psi_{i,j,k_z}(z)=\sum_m e^{ik_zmd}\psi_{i,j}(z-md), \qquad (2.25)$$

where $\psi_{i,j}(z)$ is the eigenfunction of a separate quantum well, while

$$E_{i,j}(k_z)=E_{i,j}; \qquad (2.26)$$

here $E_{i,j}$ is an energy eigenvalue in a separate quantum well.

For a doped superlattice with $d_n=d_p=d/2$ and a uniform distribution of impurities $n_D=n_A$. The periodic potential of the space charge is parabolic (2.16) with the amplitude (2.18)

$$V_0=\frac{\pi e^2 n_d d^2}{2\varkappa_0}, \qquad (2.27)$$

For a superlattice based on GaAs ($\varkappa_0=12.5$) with $n_D=n_A=10^{18}$ cm^{-3}.[6] The effective gap width in the doped superlattice (see Fig. 9) is equal to

$$E_g^{\mathrm{eff},0}=E_g^0-2V_0+E_{c,0}+E_{hh,0}. \qquad (2.28)$$

The energies of the minibands are virtually equidistant:

$$E_{i,j}=\hbar\omega_i\left(j+\frac{1}{2}\right), \qquad (2.29)$$

where ω_i is the plasma frequency of the ith type of particle,

$$\omega_i=\left(\frac{4\pi e^2 n_D}{\varkappa_0 m_i}\right)^{1/2}. \qquad (2.30)$$

In the case examined above $\hbar\omega_c=40.2$ meV, $\hbar\omega_{lh}=38.3$ meV, $\hbar\omega_{hh}=17.3$ meV.[6] Thus the effective energy gap of the doped superlattice is much smaller than the energy gap of the bulk semiconductor E_g^0 (for GaAs $E_g^0=1.52$ eV).

If the thickness of n layers or (and) the concentration in n layers is increased, then a finite two-dimensional electron density is formed in n-type layers $n^{(2)}$. Its magnitude can be determined from the condition of electrical neutrality:

$$n^{(2)}=n_D d_n-n_A d_p. \qquad (2.31)$$

The spatial distribution of the electrons $n(z)$ depends on the wave functions of the filled minibands and the number of current carriers in them $n_j^{(2)}$:

$$n(z)=\sum_j n_j^{(2)}|\psi_{c,j}(z)|^2. \qquad (2.32)$$

The densities $n_j^{(2)}$ are determined from the equality of the Fermi energies in all minibands:

$$E_{c,j}+\frac{\hbar^2}{2m_c}\cdot 2\pi n_j^{(2)}=E_{c,0}+\frac{\hbar^2}{2m_c}\cdot 2\pi n_0^{(2)} \qquad (2.33)$$

and the condition

$$\sum_j n_j^{(2)} = n^{(2)}, \tag{2.34}$$

if more than one miniband is filled; here $\psi_{c,j}(z)$ is the self-consistent solution of (2.23) and (2.25).[6]

For a doped superlattice consisting of thin doped layers of GaAs with $d_n = d_p = 40$ Å, separated by thick intrinsic layers $d_i = 360$ Å, with $n_D = n_A = 5.25\cdot 10^{10}$ cm^{-3}, the potential $V_i(z)$ is more likely to be triangular rather than parabolic, and the distances between the minibands for small j are larger than for large j.[78]

An important feature of doped superlattices is the fact that the extrema of the electron wave functions are shifted by one-half the superlattice period relative to the extrema of the hole wave functions. Therefore, analogously to type III compositional superlattices, the effective energy gap is indirect in the coordinate space. The recombination lifetimes of the current carriers can be made extremely short by proper selection of the parameters of the doped superlattice, since the overlapping of the wave functions can be made to be very small.

The long lifetimes make it possible to change easily the current-carrier density. Unlike ordinary semiconductors, where high nonequilibrium densities can be obtained only with very strong excitations, in order to create substantial deviations from the equilibrium density everywhere in a doped superlattice it is merely necessary that the generation rates be very low or the injection currents be very weak.

Equations (2.32)–(2.34) determine the filling of the minibands and the spatial distribution of the electrons for the excited state of doped superlattices also.

The negative space charge of electrons in n-type layers compensates the positive space charge of the donors, while the positive space charge of the holes in p-type layers compensates the negative space charge of the acceptors. Thus, when extra electrons and holes are introduced the self-consistent potential $V_{sc}(z)$ in Eq. (2.20) is smoothed and the effective energy gap of the doped superlattice increases[6]:

$$E_g^{\mathrm{eff},n} = E_g^0 - V_{cc}^n\left(\frac{d}{2}\right) + V_{cc}^n(0) + E_{c,0}^n + E_{hh,0}^n. \tag{2.35}$$

For small deviations from equilibrium $\Delta n^{(2)} = \Delta p^{(2)}$ [6]

$$\Delta E_g^{\mathrm{eff},n} = E_g^{\mathrm{eff},\Delta n} - E_g^{\mathrm{eff},0} = \frac{e^2 d_n}{\varkappa_0}\,\Delta n^{(2)}. \tag{2.36}$$

Another important consequence of the dependence of the self-consistent potential of the superlattice $V_{sc}(z)$ on the current-carrier density is that the distance between the minibands decreases when the population of the minibands increases, which is also brought about by the smoothing of the potential structure.

Radiative and nonradiative (Auger) recombination of electrons in n-type layers and holes in p-type layers depends on the square of the overlap integral of the corresponding envelope wave functions. For a superlattice with constant densities $n^D = n_A$ the envelope wave functions of the ground state coincide with good accuracy with the wave functions of the harmonic oscillator[6]

$$\psi_{1,0}(z) = \pi^{-1/4}\alpha^{-1/2}\exp\left(-\frac{z^2}{2\alpha_i^2}\right), \tag{2.37}$$

where

$$\alpha_1 = \hbar^{1/2}(m_1\omega_1)^{-1/2}. \tag{2.38}$$

The ratio of the radiative lifetimes in the doped superlattice $\tau_{\mathrm{nipi}}^{\mathrm{rad}}$ and the bulk crystal $\tau_{\mathrm{bulk}}^{\mathrm{rad}}$ is therefore given by

$$\frac{\tau_{\mathrm{nipi}}^{\mathrm{rad}}}{\tau_{\mathrm{bulk}}^{\mathrm{rad}}} \approx \frac{\alpha_c^2+\alpha_{eh}^2}{2\alpha_c\alpha_{eh}}\exp\frac{d^2}{4(\alpha_c^2+\alpha_{eh}^2)}; \tag{2.39}$$

if $n_D = n_A = 10^{18}$ cm^{-3}, $d_n = d_p = d/2 = 400$ Å, then

$$\frac{\tau_{\mathrm{nipi}}^{\mathrm{rad}}}{\tau_{\mathrm{bulk}}^{\mathrm{rad}}} \approx 10^{13} \tag{2.40}$$

and the radiative lifetime increases from nanoseconds to hours. If the period of the superlattice is decreased by only a factor of two, however, then

$$\frac{\tau_{\mathrm{nipi}}^{\mathrm{rad}}}{\tau_{\mathrm{bulk}}^{\mathrm{rad}}} \approx 2\cdot 10^3. \tag{2.41}$$

The nonradiative recombination time also changes analogously.[6]

Doped superlattices with adjustable electronic properties and with a large increase in the mobility of two-dimensional electrons and holes were recently synthesized.[79] This structure consists of a periodic repetition of the layers n-Al_xGa_{1-x}As–i-GaAs–n-Al_xGa_{1-x}As–p $=$ Al_xGa_{1-x}As–i-GaAs–p-Al_xGa_{1-x}As and is a hybrid of doped and compositional superlattices (Fig. 10). In this superlattice, aside from the spatial separation of electrons and holes by one-half the period, there also exists (analogously to modulation-doped type I compositional superlattices (see Fig. 7b)) a spatial separation of the free current carriers from their impurity centers.[6,7] The energy structure of this superlattice was calculated in Ref. 78.

The unusual properties of doped superlattices (an energy gap which can be varied over a wide interval, very long recombination time, etc.) are also preserved in amorphous doped superlattices. Amorphous doped superlattices make it possible to obtain new information on the properties of amorphous semiconductors,[80] for example, information about the magnitude of the gap in the density of states of the bulk amorphous semiconductor. Amorphous doped superlattices based on a-Si:H were recently synthesized.[81,82]

Calculations of the band structure of semiconductor superlattices in a magnetic field are presented in Ref. 83.

2.3. Collective excitations

In this section we shall briefly discuss the collective excitations of the one-dimensionally ordered two-dimensional

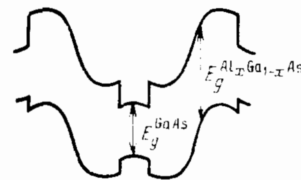

FIG. 10. Energy structure of the doped superlattice Al_xGa_{1-x}As with a semiconductor having a smaller energy gap (GaAs) in each p and n type layer.[6]

gas of current carriers in semiconductor superlattices.

In a two-dimensional electron gas the plasma frequency is $\omega_p^{(2d)} \propto k_\perp^{1/2}$ (in the limit $k_\perp \to 0$).[84] In superlattices these two-dimensional plasmons, associated with the lowest miniband, are intraband collective excitations. Collective excitations in a two-dimensional electron-hole gas were studied in Ref. 85.

An interesting characteristic feature of plasma oscillations propagating along the axis of the superlattice is the absence of Landau damping in them—the dispersion equation has a purely real solution. This is associated with the narrowness of the minibands of the energy superlattice, owing to which the spectrum of the plasma oscillations does not coalesce with the continuous spectrum—scattering of a plasmon propagating along the axis of the superlattice by a pair of single-particle excitations is forbidden by the laws of conservation of energy and momentum. The spectrum of plasma oscillations propagating along the axis of the semiconductor was calculated for high temperatures in the random-phase approximation in Ref. 86.

Collective plasma modes in the low-temperature limit were calculated in Ref. 87. For $k_z d = 0$, $k_\perp d \to 0$

$$\omega_p^2 = \frac{4\pi e^2}{\varkappa_0 d}(\alpha_e + \alpha_h), \quad \alpha_{e(h)} = \frac{n_{c(v)}^{(2d)}}{m_{c(v)}} \tag{2.42}$$

(here $n_{c(v)}^{(2d)}$ is the two-dimensional electron (hole) density), the usual three-dimensional plasmon appears. At $k_z d = \pi$, $k_\perp d \to 0$

$$\omega_{p,\,e(h)}^2 = \frac{dk_\perp^2 \pi e^2}{\varkappa_0}\alpha_{e(h)}, \tag{2.43}$$

there are two acoustic plasma modes of the electron and hole types. For $k_\perp d \gg 1$ (the quantum wells are widely separated in space)

$$\omega_{p,\,e(h)}^2 = \frac{2\pi e^2 k_\perp}{\varkappa_0}\alpha_{e(h)}, \tag{2.44}$$

there are two two-dimensional plasmons (electron and hole).

In experiments (inelastic light scattering[88]) and limit $k_z d = \text{const}$, $k_\perp d \to 0$ is realized in semiconductor superlattices; then

$$\omega_{p,\,\pm}^2 = \frac{k_\perp^2 d\pi e^2(\alpha_e^2 + \alpha_h^2)}{\varkappa_0(1 - \cos k_z d)}(1 \pm \tilde{\Delta}), \qquad \tilde{\Delta} = \left[1 + \frac{4\alpha_e\alpha_h}{(\alpha_e + \alpha_h)^2}\cos^2\frac{k_z d}{2}\right]^{1/2}, \tag{2.45}$$

and there are two plasma modes of the acoustic type.

Propagation of helicoidal waves in semiconductor superlattices, which was studied theoretically in Ref. 89 and experimentally in Ref. 90, can be used (analogously to the quantum Hall effect) to determine the fine structure constant $\alpha = e^2/\hbar c$. When the plateau in the Hall conductivity $\sigma_{xy} = je^2/h$ ($j = 1, 2, 3, \ldots$), $\sigma_{xx} = 0$ is observed, for low frequencies $\omega \ll \omega_c$ (ω_c is the cyclotron frequency) the frequency of the helicoidal waves

$$\omega_j = \frac{1}{2}\frac{c}{j\alpha}dk_z^2 \tag{2.46}$$

is independent of the magnetic field. By measuring ω_j it is therefore possible to determine the fine structure constant.[89]

The spectrum of acoustic plasmons was studied in Ref. 91 for semi-infinite type I superlattices and in Ref. 92 for type II superlattices. The possibilities of using acoustic plasmons to perform studies in the submillimeter range are discussed in Ref. 93.

A detailed theoretical study of the electronic collective excitations in semiconductor superlattices is carried out in Ref. 94.

The center of mass of an electron and a hole, excited in a type I compositional semiconductor, moves freely in the plane of the layers. Because the motion of the current carriers is spatially restricted by the dimensions of the quantum well, the binding energy of the exciton in the superlattice is higher than in the bulk semiconductor. If the height of the quantum barrier is infinite, then, as the width of the quantum well $d_{\rm I}$ decreases, the binding energy of the exciton in type I superlattices increases monotonically from the binding energy of the three-dimensional exciton in the limit $d_{\rm I} \to \infty$ up to the binding energy of the two-dimensional exciton (four times higher) in the limit $d_{\rm I} \to 0$ (see, for example, Ref. 95).

Taking into account the finite height of the potential barrier lowers the binding energy of the exciton. When the height of the energy barrier is constant, the binding energy of the exciton is a nonmonotonic function of $d_{\rm I}$.[96]

Type I compositional superlattices, whose layers have substantially different dielectric permittivities, have interesting characteristics. If the parameters of these superlattices satisfy the conditions

$$d_{\rm I} \ll a_{2d}, \quad d_{\rm II} \gg \eta a_{2d}, \quad \eta \ll 1, \quad \eta d_{\rm I} \ll d_{\rm II} \ll \frac{d_{\rm I}}{\eta}, \tag{2.47}$$

where $\varkappa_{\rm I(II)}$ are the dielectric permittivities of the quantum well (barrier),

$$\eta = \frac{\varkappa_{\rm II}}{\varkappa_{\rm I}}, \quad a_{2d} = \frac{\varkappa_{\rm I}\hbar^2}{2me^2}, \tag{2.48}$$

and m is the reduced effective mass of the electron and hole, then the energy spectrum of the exciton has the following form[97]:

$$E_{x,\,j} = -\frac{e^2}{\varkappa_{\rm I} d_{\rm I}}\left[\ln\left(\frac{8d_{\rm II}}{\eta a_{2d}}\right) - 2C + 2\gamma_j\right], \tag{2.49}$$

where $C = 0.577\ldots$ is Euler's constant and γ_j are constants determined in Ref. 98; thus $\gamma_0 = -0.525$. When $\eta = 0.001$, $d_{\rm I} = 0.1\,a_{2d}$, $d_{\rm II} = a_{2d}$, $E_{x,0} = 45\,E_{2d}$, and when $\eta = 0.001$, $d_{\rm I} = 0.1\,a_{2d}$, $d_{\rm II} = a_{2d}\,E_x,0 = 70\,E_{2d}$ ($E_{2d} = 2e^4m/\varkappa_{\rm I}^2\hbar^2$), while in a film (a double heterojunction) of thickness $d_{\rm I}$ for the same value of η $E_{x,0} = 100\,E_{2d}$. Thus the binding energy of an exciton in such superlattices is much higher than that of a two-dimensional exciton (E_{2d}), but lower (though it is of the same order of magnitude) than in a thin film[98] for the same values of η and $d_{\rm I}$ and approaches the binding energy in a thin film as $d_{\rm II}$ increases.

The binding energy of an exciton in type III compositional superlattices (with spatial separation of electrons and holes) was calculated in Refs. 95 and 99. It turned out that the increase in the binding energy of the exciton accompanying a decrease in the superlattice period is small.

The binding energy of the exciton in doped superlattices was calculated in Ref. 100. For strong doping the excitons

are quasi-two-dimensional, while for weak doping they are almost three-dimensional. The case when the period of the doped superlattice is of the order of the radius of the three-dimensional exciton $d \lesssim a_{2d} = 2a_{2d}$ is especially interesting; then when the doping level is lowered, the binding energy at first increases and then decreases to the three-dimensional value $E_{3d} = E_{2d}/4$.

3. OPTICAL PROPERTIES

The optical properties of all semiconductor superlattices are the same in the range of frequencies below the threshold of intrinsic absorption in the constituent bulk semiconductors of the superlattice. For frequencies above the threshold of intrinsic absorption, however, the optical properties of type I compositional superlattices differ substantially from those of type III compositional superlattices and of doped superlattices. A quite detailed theoretical study of the optical properties of semiconductor superlattices is carried out in Ref. 19.

3.1. Intraband processes

The optical properties of semiconductor superlattices in the range of frequencies below the threshold of intrinsic absorption are markedly anisotropic. If the electric field of the light wave is perpendicular to the axis of the superlattice, then the usual absorption by free current carriers is observed. Only light polarized parallel to the axis of the superlattice can excite electronic transitions between different minibands. Because of this, the frequency dependence of the coefficient of absorption consists of a series of bands, within which the magnitude of the absorption coefficient is much higher than for absorption by free carriers. The position and width of the bands are determined by the nature of the miniband spectrum, so that they can be easily changed by changing the lattice parameters.

Transitions between states with different parity are allowed. The coefficient of absorption for the bottom miniband of the conduction band is equal to[19]

$$\alpha(\omega) = \begin{cases} \dfrac{4\pi e^2 \omega n}{Nc} |z_{0j}|^2 [\Delta_{0j}^2 - (\hbar\omega - E_{0,j})^2]^{-1/2}, \\ |\hbar\omega - E_{0,j}| \leqslant |\Delta_{0,j}|, \\ 0 \\ |\hbar\omega - E_{0,j}| > |\Delta_{0,j}|, \end{cases} \tag{3.1}$$

where

$$\Delta_{0,j} = \Delta_{c,j} - \Delta_{c,0}, \quad E_{0,j} = E_{c,j} - E_{c,0}, \quad j = 1,3,5,\ldots, \tag{3.2}$$

N is the index of refraction of the given semiconductor, z_{0j} is the matrix element of the coordinate between the states of the bottom and the jth minibands, and $|z_{0j}| \sim d$. Intraband processes are reviewed in detail in Ref. 19.

Intraband transitions in the valence and conduction bands were observed in the semimetallic type II superlattices InAs-GaSb in the absorption of far-infrared radiation in a magnetic field.[101–102] For each frequency of infrared radiation, oscillations of the absorption as a function of the magnetic field, linked to transitions between Landau sublevels, were observed. These experiments made it possible to determine the position of the minibands and their width, and they also confirmed the semimetallic nature of type II superlattices.

Intraband transitions in a magnetic field have also been observed in the stressed superlattices $PbTe\text{-}Pb_{1-x}Sn_xTe$.[103]

Light absorption by free electrons can be used in a photodetector of 4-μm infrared radiation, built on the basis of the superlattices $GaAs\text{–}Al_xGa_{1-x}As$. In this superlattice the absorption associated with the phonons is three to five times higher than in bulk GaAs; in addition, zero-phonon absorption of radiation by free carriers, which increases the absorption even more, can also occur in superlattices.[104] The absorption of light by free carriers associated with scattering by optical phonons was calculated for compositional superlattices in Ref. 105.

3.2. Interband transitions. Compositional superlattices

Quantum effects associated with the two-dimensional motion of current carriers in the quantum wells of type I compositional superlattices are clearly observed in their optical properties.

The wave functions of the current carriers in semiconductor superlattices are products of the envelope functions $\psi_{c,j}(z)$, $\psi_{v,j}(z)$ and the volume Bloch functions $u_c(\mathbf{r})$, $u_v(\mathbf{r})$. The interband dipole matrix elements will therefore be large only for transitions between electron and hole minibands with the same miniband numbers j. This is linked to the fact that the overlapping between any other envelope functions is very small.

This selection rule makes possible the introduction of the total density of states for each pair of minibands with the same j indices $N_{cv}(E)$ (neglecting the width of the minibands).

In the effective mass approximation $N_{cv}(E)$ is constant because of the quasi-two-dimensionality of the system in the intervals

$$E_{c,v}^{(j-1)} < E < E_{c,v}^{(j)}, \tag{3.3}$$

where

$$E_{c,v}^{j} = E_{c,j} - E_{v,j}. \tag{3.4}$$

In the single-particle approximation the coefficient of optical absorption $\alpha(\hbar\omega)$ is proportional to $N_{cv}(E)$, but the presence of quasi-two-dimensional excitons gives rise to the appearance of exciton absorption peaks at energies somewhat lower than E_{cv} (Fig. 11).

We note that the full energy spectrum of the superlattice (2.3) does not contain new forbidden bands. The presence of minigaps in $E_j(k_z)$ only indicates the purely two-dimensional character of the motion of the current carriers in these regions.

Experimental studies of the absorption of light in semiconductor superlattices $GaAs\text{–}Al_xGa_{1-x}As$[106,107] have qualitatively confirmed the expected behavior of the absorp-

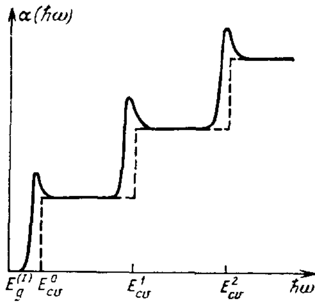

FIG. 11. Schematic dependence of the coefficient of interband absorption $\alpha(\hbar\omega)$ in type I compositional superlattices (solid curve).[6] The broken curve corresponds to the single-particle approximation (neglecting exciton effects).

tion spectra. This was the first experimental confirmation of the applicability of the effective-mass approximation for the calculation of semiconductor superlattices (Fig. 12).

It turns out[106,107] that if the thickness of the GaAs layer in the type I compositional superlattices GaAs–$Al_xGa_{1-x}As$ becomes of the order of or less than the Bohr radius of the exciton in bulk GaAs, then the binding energy of the excitons increases substantially. This is linked to the spatial confinement of the wave function of the exciton, which becomes increasingly more two-dimensional.[108] Because of the increase in the binding energy, excitons can be observed at higher temperatures (including also at room temperatures) in the superlattices GaAs–$Al_xGa_{1-x}As$ than in bulk GaAs.[108,109]

At room temperatures the saturation of optical absorption in the superlattices GaAs–$Al_xGa_{1-x}As$ is achieved with intensities which are three times lower than in the bulk GaAs.[109] The high nonlinearity of the coefficient of absorption makes it possible to observe optical bistability at room temperature and with low pumping powers.[110]

Type I compositional superlattices of the HgTe-CdTe type can be used to detect infrared radiation for wavelengths in the range 8–12 μm. In these superlattices it is much easier to select the parameters determining the absorption band of light, while the tunneling currents are much lower (therefore, the sensitivity is higher) than in the alloys $Hg_xCd_{1-x}Te$.[35,51]

In GaAs–$Al_xGa_{1-x}As$ superlattices, both the absorption edge and the long-wavelength boundary of the radiative

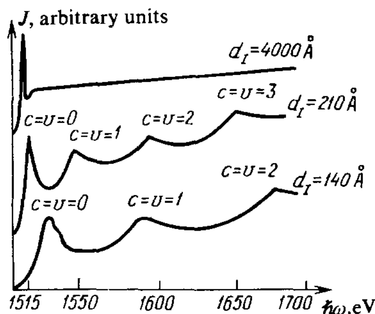

FIG. 12. Absorption spectra of GaAs-$Al_{0.2}Ga_{0.8}As$ superlattices observed at 2 K.

recombination spectrum of electrons and holes shift toward higher photon energies as compared with bulk GaAs. The magnitude of this shift depends primarily on the thickness of the GaAs layer (d_1) (9.7). The frequency of the light emitted by the semiconductor lattice can be 1.4–1.5 times higher than in the bulk semiconductor.[111]

The allowed transitions between minibands of the valence band (heavy holes) and of the conduction band with $j = 0$, 1, and 2 have been observed in the spontaneous emission of the superlattices GaAs–$Al_xGa_{1-x}As$. The position of the observed lines is in good agreement with the calculations of the minibands, taking into account the finite depth of the quantum wells and the nonparabolicity of the conduction band. When the excitation intensity was increased, a change linked with the filling of minibands was observed in the emission spectra.[112]

The shift in the energies of photons emitted by type I superlattices toward energies higher than the energy gap of the bulk semiconductor makes GaAs and InP the basic technological materials for the layers corresponding to the quantum wells. The wavelength of GaAs-based light-emitting devices can be shifted into the visible part of the energy spectrum with wavelengths shorter than 7000 Å. The wavelengths of light-emitting devices using InP-$In_xGa_{1-x}As$, InP-$In_xAl_{1-x}As$ superlattices can be less than 1 μm, which makes it possible to circumvent the technological difficulties associated with the use of the quaternary compounds $In_xGa_{1-x}As_yP_{1-y}$.[111]

An investigation of the emission and absorption spectra of optically excited superlattices GaAs–$Al_{0.3}Ga_{0.7}As$ has shown that the emission and absorption spectra of superlattices are substantially different from the spectra of bulk GaAs.[113] Radiative recombination in straight-band semiconductors is determined primarily by impurity radiation—pair recombination of free and bound current carriers (free electron—neutral acceptor or free hole—neutral donor) and by radiation from bound excitons. The intrinsic recombination of excitons in straight-band semiconductors is small. The most significant difference between the optical spectra of superlattices and the spectra of bulk semiconductors is the weakness of impurity transitions in superlattices. For example, in the superlattice GaAs (52 Å)–$Al_{0.42}Ga_{0.58}As$ (176 Å) the intensity of recombination radiation of free excitons is 2.5 orders of magnitude higher than the impurity radiation (free exciton—neutral acceptor).[111] In superlattices with very thick layers GaAs ($\gtrsim 1000$ Å), however, some lines which are typical for bulk GaAs begin to appear.[113,114] This difference in the optical properties of superlattices with different layer thicknesses indicates that the spatial restriction of the wave functions of the current carriers by the dimensions of the layer in superlattices with a period > 200 Å plays the main role in emission and absorption processes.

The first consequence of this restriction is the dependence of the binding energy of the impurity on the distance to the interface, when this distance becomes of the order of the Bohr radius of the impurity (105 Å for donors and 25 Å for acceptors).[115,116] This gives rise to the formation of impurity bands.[115–117]

The second consequence of the spatial limitation is the decrease in the oscillator strength of the impurity associated with the change in the symmetry of its wave function from 1s symmetry in the bulk semiconductor to 2p symmetry, when the impurity is located on the interface.[113,117]

Another factor which has a significant effect on the emission spectra of compositional semiconductors is the presence of perfect (sharp) interfaces between the constituents of the superlattice.[10,111] The width of the emission lines of the excitons is correlated with fluctuations of the interfaces. Thus, for example, the existence of a Stokes shift (of the order of several meV in type I superlattices InP–$In_{0.43}Ga_{0.57}As$) can be explained by the trapping of an exciton by island defects in the interfaces with a thickness of the order of one atomic layer (2.86 Å) and a diameter of ~ 100 Å.[108] (The mechanism of this process is studied in Refs. 33 and 118a.)

The spectra of superlattices with sharp interfaces are characterized by very narrow emission lines (1–2 meV wide at 15 K). The best samples exhibit additional emission lines, shifted toward lower energies by 1 meV, which are linked to the emission from biexcitons.[8,118b]

The spatial restriction of the motion of the current carriers has an important effect on the electroabsorption of light in the superlattices GaAs–$Al_xGa_{1-x}As$.[119,120] The Stark effect in superlattices differs substantially from the Stark effect in atoms and in bulk semiconductors. The exciton resonance in electroabsorption of superlattices for electric fields oriented parallel to the axis of the superlattice remains allowed, even if the Stark shift is much (by a factor of 2.5) larger than the binding energy of the exciton in the absence of an electric field, for electric fields $E_z \gtrsim 50\, E_i$ ($\sim 10^5$ V/cm), where

$$E_i = \frac{E_x}{8a_x} \tag{3.5}$$

is the classical ionization field,[120] and E_x and a_x are the binding energy and radius of the exciton in the absence of an electric field. The existence of exciton absorption in such strong electric fields is explained by the fact that the walls of the quantum wells prevent carriers from escaping from the quantum wells when they are ionized by an electric field. In addition, the small—as compared with the radius of the exciton in bulk GaAs (~ 300 Å)—width of the quantum wells (~ 100 Å) gives rise to the fact that the electron-hole interaction is quite strong, even though it is weakened by the strong electric field.[120] The presence of a large (~ 10 meV) Stark shift of excitons in GaAs–$Al_xGa_{1-x}As$ superlattices in electric fields of $\sim 1.6\cdot10^4$ V/cm at room temperature can be used in fast-response optical modulators.[119]

The electroluminescence of superlattices GaAs–$Al_xGa_{1-x}As$ also exhibits interesting features.[121]

The study of the magnetooptics of excitons in the superlattices GaAs–$Al_xGa_{1-x}As$ showed that the diamagnetic shift of an exciton with a heavy hole is much larger than that of an exciton with a light hole.[122] The binding energy of the excited states of the exciton depends more strongly on the magnetic field than does the energy of the ground state.[123] When the magnetic field is increased, the lifetime of the exciton decreases. This is linked to the fact that the localization of the exciton increases.[124] Extrapolation of the experimental results of magnetooptics to zero magnetic field has shown that when the width of the quantum well decreases, the exciton changes from a three- to a two-dimensional exciton.[122] The theory of magnetoabsorption of light is given in Ref. 125a.

The observation of a new narrow (~ 1 meV) photoluminescence line of the superlattices GaAs–$Al_xGa_{1-x}As$ with very strong selective excitation was reported in Ref. 125b. This line was red-shifted relative to the exciton line by ~ 6 meV. The integrated intensity of this line changed more rapidly than the square of the intensity of the exciton line; in addition, when the temperature is raised from 1.9 to 45 K its intensity drops, while the intensity of the exciton line increases. This line apparently corresponds to the emission from an electron-hole liquid.[126a]

The study of the kinetics of type I superlattices has attracted a great deal of interest in recent years.[124,126b-129a] The radiative lifetimes, the tunneling time from the region of the quantum barrier into the region of the quantum well, the screening time of excitons, and so on have been determined. Thus, for example, the transition of current carriers from $Al_{0.4}Ga_{0.6}As$ barriers 176 Å wide into GaAs quantum wells 52 Å wide occurs ballistically within a time of 10^{-13} sec.[128]

An investigation of the kinetics of cathodoluminescence of the superlattices GaAs–$Al_xGa_{1-x}As$[111] showed that the free-exciton lifetimes $\tau(d_1)$ decrease with the width of the quantum well d_1; thus $\tau(113\ \text{Å})/\tau(52\ \text{Å}) = 1.8$. Calculations[95,111] show that the exciton lifetime decreases by a factor of ~ 12 in going from a three-dimensional layer to a monolayer. This decrease is explained by the fact that the recombination probability is proportional to the square of the exciton radius, which decreases with the width of the quantum well.

Resonance Raman scattering in GaAs–$Al_xGa_{1-x}As$ superlattices has made possible the observation of delocalized excitons—excitons consisting of electrons and holes belonging to minibands, lying far above the superlattice potential. These excitons, unlike the quasi-two-dimensional excitons with lower energies, whose envelope functions approach zero at the interfaces, are characterized by envelope functions such that the existence of sharp interfaces does not destroy the correlations between the electron and hole forming the exciton.[129b]

Lasers based on GaAs–$Al_xGa_{1-x}As$ superlattices[130–132] have much better characteristics than double-heterojunction lasers. The minimum value of the threshold current for a double-heterojunction laser is ≈ 500 A/cm^2, while for a superlattice laser the minimum value is ≈ 160 A/cm^2.[133] Superlattices are the best three-dimensional laser structures because of the higher probability of radiative transitions and the significantly lower trapping of current carriers by impurities and defects in them. In addition, the temperature dependence of the threshold current in superlattice lasers is much weaker than in double-heterojunction lasers,[134] which is apparently linked to the increased trapping of current carriers.[135] A detailed review of the advan-

tages of using compositional superlattices as light-emitting devices is given in Ref. 11.

The optical properties of type III semiconductor superlattices (see Fig. 5) (InAs-GaSb with periods of 30–60 Å, when these superlattices exhibit semiconducting properties) also exhibit interesting characteristics.[136]

InAs-GaSb superlattices are similar to doped superlattices (see Fig. 9) and are characterized by an indirect energy gap in coordinate space. The selection rules[4] for optical transitions in these superlattices for wave vectors of the initial state $\mathbf{k}$ and the final state $\mathbf{k}'$ give $\mathbf{k} = \mathbf{k}'$. This selection rule allows transitions between minibands of the valence band and of the conduction band with different miniband numbers j. In this case the coefficient of absorption will have the following form[4]:

$$\alpha(\hbar\omega) \sim \sum_{j,\,j'} \int \mathrm{d}\mathbf{k} \left| \int_0^d \mathrm{d}z \psi^*_{\mathrm{c},\,j}(z)\, \psi_{\mathrm{v},\,j'}(z) \right|^2 \times \delta\left[E_{\mathrm{c},\,j}(\mathbf{k}) - E_{\mathrm{v},\,j}(\mathbf{k}) - \hbar\omega\right]. \quad (3.6)$$

The matrix elements for minibands with low numbers are very small, since the envelope wave functions $\psi_{c,j}(z)$ and $\psi_{v,j'}(z)$ are concentrated in different spatial regions. In order for the absorption between these minibands to be appreciable, the layers must be thin enough for the wave functions to penetrate appreciably into the neighboring regions. Numerical calculations have shown that even under favorable conditions the absorption is much weaker than in bulk semiconductors and transitions with $j = j'$ and $j \neq j'$ make comparable contributions. The energy difference between the maximum of the valence band of GaSb and the minimum of the conduction band of InAs, which turned out to be equal to 150 meV, was determined from a comparison of the theoretical and experimental results.[4]

The optics of stressed superlattices[51,54,104] exhibits a number of interesting features. The study of optical absorption in stressed superlattices showed that the stresses induced by the mismatch of the lattice constants change the mutual position of the excitons, associated with light and heavy holes, which is in good agreement with the simple effective-mass theory.[51] The high luminescence level, especially of stimulated emission in stressed superlattices, indicates that the density of defects at the interfaces is low.[54,55]

Saw-tooth superlattices are characterized by interesting transient properties. The absence of mirror symmetry gives rise to the appearance of macroscopic electric polarization over distances much larger than the superlattice period. Electron-hole pairs excited in such a superlattice by a short light pulse separate within 10^{-13} sec from the holes and migrate into the location with the smaller gap (we are considering p-type superlattices in which the valence band is not modulated), creating a dipole moment which then slowly decays because of hole drift.[70]

The optics of amorphous superlattices is studied in Ref. 72, where the dependence of the optical gap on the width of the energy well (on the thickness of the *a*-Si:H layer) was determined. The study of the optical properties of amorphous superlattices offers a new possibility for studying amorphous semiconductors.

3.3. Interband transitions. Doped superlattices

The optical properties of doped superlattices are determined by the spatial separation of electrons and holes. The tunability of the energy structure of doped superlattices has the consequence that it is possible to alter the spectrum and the radiation intensity. It is of special interest to study stimulated recombination radiation of electrons and holes. This is linked to the fact that because of the long lifetime of current carriers (2.39)–(2.41) quite weak excitations are required to create an inverted population in a wide energy range. In addition, the radiation spectrum of a doped superlattice can differ substantially from the spectrum of a bulk semiconductor (2.28).

Light absorption in a doped superlattice is possible if the energy of the photons exceeds the effective energy gap (2.28). The overlapping of the wave functions of the lowest minibands of the conduction band and the highest minibands of the valence band is small, and therefore the absorption coefficient is also small.

The absorption coefficient of doped superlattices increases in a jump-like manner, analogously to the absorption coefficient of a compositional superlattice, reflecting the jumps in the two-dimensional density of states.[6]

The electrons and holes generated by the light occupy in the doped superlattice the lowest minibands of the conduction band and the highest minibands of the valence band. The spatial separation of the maxima of the valence band and the minima of the conduction band (see Fig. 9) almost suppresses the recombination of current carriers. The recombination lifetimes, determined from the decay of the photocurrent after illumination, for effective energy gaps (2.35) less than 0.2 eV are equal to $\sim 10^3$ s.[137]

Because of the fact that most current carriers relax to the band extrema and do not recombine, the current-carrier density increases proportionally to the illumination time. The excess current carriers compensate the space charge of the impurity centers, as a result of which the amplitude of the superlattice potential decreases, while the effective energy gap (2.36) increases.[6,78]

In its turn the absorption coefficient depends on the magnitude of the effective energy gap. As a result, self-transparency can be produced in doped superlattices,[12] since the stationary value of the coefficient of absorption, which corresponds to equilibrium between generation and recombination of current carriers, depends not only on the frequency but also on the intensity of the incident light.

An interesting feature of the tunable absorption coefficient is the oscillatory dependence of the coefficient of absorption on the magnitude of the effective energy gap at a fixed photon frequency.[6] If the effective energy gap increases, then the superlattice potential becomes flatter and the overlapping of the wave functions of the electrons and holes (and therefore the coefficient of absorption also) increases. The absorption coefficient, however, drops sharply,

if one of the transitions becomes energy-forbidden as $E_g^{\text{eff},n}$ increases:

$$E_{c,j} - E_{v,j'}|_{E_g^{\text{eff},n}} = \hbar\omega \qquad (v = \text{lh, hh}). \tag{3.7}$$

The oscillatory behavior intensifies, if the distance between the minibands increases and if not too many minibands contribute to the absorption. The observation of this effect requires doped superlattices with a high impurity concentration and not very large period.

If the doped superlattice has a long period and a moderate doping level, then the number of minibands participating in the absorption is so large that the stepped quantum structure is smoothed out. In this quasiclassical limit, when the photon energy is increased the absorption corresponds to transitions between minibands with increasing numbers, in which the overlapping of the wave function becomes increasingly larger. Thus for photon energy of the order of the energy gap of an unmodulated semiconductor E_g^0 the situation is very reminiscent of the Franz-Keldysh effect[138]—the coefficient of absorption decreases exponentially with the photon energy for photon energies less than E_g^0. The finite absorption of light for photon energies less than E_g^0 has been observed in doped superlattices.[139]

The dependence of the absorption coefficient on the width of the effective energy gap and the very long lifetime give rise to large nonlinearities in the optical properties of doped superlattices already at low excitation densities. At a fixed frequency of the light, a large change is observed in the absorption of the light as the intensity of the light is changed. This nonlinearity differs from the nonlinearity of the optical absorption of compositional superlattices, which is associated with miniband filling or exciton screening.[109] The self-transparency of doped superlattices has practical applications. The large changes in the optical path achieved at moderate intensities give rise to optical bi- and multistability.[141]

The absorption of phonons with energy greater than the energy gap of an unmodulated semiconductor E_g^0 is a "vertical" process in both the momentum and coordinate spaces. In this case the generation of electron-hole pairs remains practically unchanged along the axis of the superlattice. Relaxation of current carriers in momentum and coordinate space then occurs. The relaxation of current carriers is a much faster process ($\tau^{\text{rel}} \sim 10^{-12}$ s) than radiative recombination ($\tau^{\text{rad}} \sim 10^{-9}$ s). This is also valid in doped superlattices, since electrons (holes) drift in n(p) type layers because of relaxation processes.[141] Thus the spatial separation of electrons and holes in a doped superlattice substantially lowers the probability for finding a partner for a vertical recombination process with $\hbar\omega \approx E_g^0$.

The equilibrium state of photoluminescence is determined from the condition that the process of recombination through the indirect effective energy gap in the coordinate space $E_g^{\text{eff},n}$ and the process of generation of electrons and holes accompanying the absorption of light be balanced.

The tunability of $E_g^{\text{eff},n}$ of a doped superlattice was vividly demonstrated in an experimental study of photoluminescence.[141–147] The position of the emission line red-shifted substantially (by more than 200 meV) when the radiation intensity was lowered. Analogous results were also obtained in an experimental study of electroluminescence.[145,147]

Direct spectroscopic information on the energy structure of doped superlattices can be obtained from inelastic light scattering.[142,143,146] Transitions between the first, second, and third minibands of the conduction band have been observed. Experiments on Raman scattering of light have shown that when the excitation intensity is increased, the superlattice potential is smoothed and the system becomes increasingly more three-dimensional.

The optics of amorphous doped superlattices exhibits interesting features.[82]

4. ACOUSTICAL PROPERTIES

In this section we shall examine the much less well studied (as compared with the optical properties) acoustical properties of semiconductor superlattices.

Because of the new periodicity of semiconductor superlattices, gaps with wave vectors $q_z = (2j+1)\pi/d$ form in the phonon spectrum. This is manifested in the selective reflection of phonons by the superlattice. Phonons with wavelengths λ are reflected most strongly (the Bragg condition)

$$\lambda = 2d. \tag{4.1}$$

The filtering action of semiconductor superlattices GaAs–$Al_{0.5}Ga_{0.5}As$ has been observed experimentally and can be exploited to build a phonon spectrometer. Thus the superlattice GaAs–$Al_{0.5}Ga_{0.5}As$ with a period of 122 Å is a phonon filter for the frequency $2.2 \cdot 10^{11}$ Hz with a line width of $0.2 \cdot 10^{11}$ Hz. It is interesting to note that high-frequency phonons with wavelengths of ~ 100 Å pass without appreciable attenuation through hundreds of interfaces in compositional superlattices, which confirms the near ideality of the interfaces obtained with the help of molecular-beam epitaxy.[148]

Phonons with the wave vectors $q_z = 2\pi j/d$ at the center of the new Brillouin zones appear in the resonant Raman scattering. New sharp lines of longitudinal acoustic phonons with frequencies of 63.1 cm^{-1} and 66.9 cm^{-1} have been observed in the superlattice GaAs-AlAs with a period of 25 Å. These modes correspond to oscillations of the superlattice layers relative to one another. The study of the line shape shows that the thickness of the superlattice layers is the same to within $\sim 2\%$, while the phonon scattering time is $> 10^{-11}$ s.[149]

The dispersion curves of acoustic phonons have been determined from the Raman scattering of light in GaAs–$Al_xGa_{1-x}As$ superlattices with a large period[150] and GaAs-AlAs superlattices with a period of 12–3000 Å.[151]

The periodic alternation of the spatially distributed charge layers in the type II compositional superlattices (InAs-GaSb) or nonuniformly doped type I superlattices (GaAs–$Al_xGa_{1-x}As$) can be used for direct electromagnetic generation of high-frequency acoustic waves with the frequencies

$$\omega = j \cdot \frac{2\pi s}{d}, \quad j = 1, 2, 3, \ldots, \tag{4.2}$$

where s is the sound velocity. If $d = 200$ Å and $s = 4 \cdot 10^5$ cm/sec, then the resonance frequency of the generated sound is $\omega \sim 10^{11}$ Hz.[152]

The magnetophonon effect—resonance scattering of electrons by optical phonons, when the distance between the Landau levels is equal to the energy of the longitudinal optical phonon—has been observed in $Ga_{1-x}In_xAs$–InP superlattices. It turned out that electrons in the quantum well $Ga_{1-x}In_xAs$ are scattered by both longitudinal optical phonons of the "GaAs type" and by InP optical phonons. The dependence of the frequency of optical phonons on the thickness of the layers $Ga_{1-x}In_xAs$ was measured.[153]

A quite detailed theoretical study of the phonon spectrum of semiconductor superlattices has been made. The characteristic features of the phonon spectrum of superlattices at high temperatures were calculated in Ref. 154. The spectrum of phonons on the interfaces of superlattices consisting of polar semiconductors was studied in Refs. 155 and 156. The absorption of sound in semiconductor superlattices was studied in Refs. 157 and 158. It was shown that a phonon instability, giving rise to sound amplification, can occur in a quantizing electric field. Gigantic oscillations of the sound absorption in a magnetic field were studied in Refs. 159 and 160. A detailed analysis of these studies falls outside the scope of this review.

5. TRANSPORT PHENOMENA

In this section we shall briefly study transport phenomena in semiconductor superlattices. Quantum transport phenomena in semiconductor superlattices are reviewed in detail in Ref. 161.

One reason for the increased interest in semiconductor superlattices is the significant nonlinearity of their transport properties, owing to the existence of very narrow minibands in the energy spectrum of such superlattices.

The transport properties of semiconductor superlattices are strongly anisotropic. The mobility of current carriers in the layers of the superlattice is of the order of their mobility in the bulk semiconductor with the same impurity concentration. The motion of current carriers along the axis of the superlattice requires that a potential barrier—the superlattice potential—be overcome.

5.1. Conductivity

One of the most interesting transport properties of semiconductor superlattices is the negative differential conductivity—the existence of a descending section on the current-voltage characteristic.[13]

In a strong static electric field E_z oriented parallel to the axis of the superlattice the motion of the current carriers is finite—they undergo oscillations with the Stark frequency

$$\Omega = \frac{eE_z d}{\hbar}, \tag{5.1}$$

and the current vanishes.

A current arises solely because of the scattering of current carriers, which is analogous to transport phenomena in bulk semiconductors in a strong magnetic field or in a high-frequency electric field, when the current (see, for example, Ref. 162)

$$I \backsim \frac{E_z\tau}{1+\omega^2\tau^2}, \tag{5.2}$$

where τ is the characteristic relaxation time and ω is the cyclotron frequency in the case of a magnetic field or the frequency of the electric field. It follows from (5.2) that $I \to 0$ in the limit $\omega\tau \to \infty$. For semiconductor superlattices the Stark frequency Ω (5.1) must be used for ω, and $I \to 0$ in the limit $\Omega\tau \to \infty$ (for Stark frequencies less than the width of the miniband).

Thus when the volume collision frequency is quite low the current carriers in an external electric field oriented parallel to the axis of the superlattice undergo Bragg reflection from the boundaries of the allowed minibands and undergo an oscillatory motion with the Stark frequency Ω.

This behavior of the current carriers can be easily explained by the fact that in the periodic potential of the superlattice the energy of their motion along the superlattice is a periodic function of the quasimomentum with a period $2\pi\hbar/d$ (2.4). In the presence of a uniform electric field E_z the quasimomentum of the current carriers is a linear function of time,

$$p_z(t) = p_z(t_0) - eE_z(t - t_0), \tag{5.3}$$

and the energy $E(p_z)$ and velocity

$$v_z(p_z) = \frac{dE(p_z)}{dp_z} \tag{5.4}$$

oscillate with the period

$$T = \frac{2\pi\hbar}{eE_z d} = \frac{2\pi}{\Omega}. \tag{5.5}$$

The velocity averaged over a period is therefore equal to zero and the electron motion is purely oscillatory. The turning points correspond to Bragg reflections. Such oscillations are not observed in bulk solids, because the time between collisions $\tau < T$ and collisions force the current carriers to be located always in the region of low quasimomenta near the bottom of the miniband. Interacting with an electromagnetic field, an oscillating electron will emit or absorb at a frequency which is equal to or is a multiple of the Stark frequency Ω (5.1). Thus in the presence of a uniform electric field E_z oriented along the superlattice axis the energy miniband splits into a collection of equidistant levels separated by the interval $eE_z d$. These levels correspond to wave functions shifted by the period of the superlattice, since in the presence of such a shift the potential changes by $eE_z d$.[163] The response of the electrons in the superlattice is strongly nonlinear, if the momentum imparted by the electric field is comparable to $\hbar/d$. Therefore, the critical value of the field E_z^*, in which the nonlinear conductivity is comparable to the linear conductivity, is given by

$$E_z^* \approx \frac{\hbar\,|\,\omega + i\tau^{-1}\,|}{ed}; \tag{5.6}$$

here ω is the frequency of the electric field and τ is the characteristic relaxation time. Because of the fact that the period of the superlattice is quite large, E_x^* is much smaller in su-

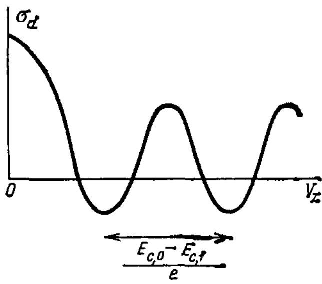

FIG. 13. Schematic dependence of the differential conductivity σ_d of GaAs-AlAs superlattices on the applied voltage V_z.[14] The period of the oscillations corresponds to the distance between the first and second minibands of the conduction band.

perlattices than in uniform crystals. Thus if $d = 200$ Å, $\tau^{-1} < \omega = 10^{-12}$ s^{-1}, then $E_z^* \approx 300$ V/cm.[164]

In systems exhibiting Bloch oscillations there exists a number of conductivity anomalies. Historically it is precisely the possibility of observing such phenomena (in particular, the negative differential conductivity in compositional superlattices[12]) that motivated experimenters to create semiconductor superlattices.

The experimental study of transport phenomena in superlattices and especially of the nonlinear properties can in its turn give valuable information on the band structure and scattering of current carriers in superlattices.[165] It is of great interest to study the high-frequency effects: 1) the peculiarities of the frequency dependence of the differential conductivity, owing to the Stark resonance[166,167]; 2) the bleaching of the medium induced by an intense monochromatic field[168]; 3) the oscillatory character of the absorption of intense electromagnetic waves[169]; 4) the oscillations of the static conductivity in the presence of an intense electromagnetic field and the concomitant effect of absolute negative conductivity[164,170–172]; 5) the photoeffect (radioelectric effect)—entrainment of electrons by an intense electromagnetic wave.[173,174]

The conductivity of semiconductor superlattices has been studied in detail theoretically.[13,20,162–178] A detailed examination of these studies falls outside the scope of this review (see, for example, the reviews given in Refs. 6 and 19 as well as the review of the motion of current carriers along interfaces given in Ref. 179).

Negative differential conductivity along the axis of the superlattice and the concomitant current oscillations have been observed in the superlattices GaAs-AlAs[180] (Fig. 13) as well as in the study of photocurrents in GaAs–$Al_xGa_{1-x}As$ superlattices.[181]

The conductivity in the plane of the layers of amorphous superlattices a-Si: H–a-$Si_{1-x}N_x$:H is distinguished by interesting features. The very low resistance in these superlattices is determined by the transport of electrons from the donor centers in a-$Si_{1-x}N_x$:H layers into a-Si:H layers. The amorphous superlattices a-Si:H–a-$Si_{1-x}N_x$:H are characterized by a high photoconductivity.[73]

Negative differential conductivity and the concomitant current oscillations were also observed in the study of transport phenomena in a direction perpendicular to the axis of the superlattice in compositional superlattices GaAs–$Al_xGa_{1-x}As$. This effect is the analog of the Gunn effect in coordinate space and is explained by heating of the electrons by the electric field and the transition of hot electrons with an energy of the order of the superlattice potential from GaAs layers into $Al_xGa_{1-x}As$ layers. The electron mobility is significantly lower in these layers and the electrons are retarded. As a result of this, the current drops when the electric field is increased.[82]

An interesting feature of doped superlattices is that the electron and hole contribution to the conductivity along the layers can be completely separated from one another by using separate electrodes. Electrodes of the $n^+(p^+)$ types (strongly doped semiconductor of the n(p) type) form a resistive contact with all layers of the n(p) type and a blocking pn contact with all layers of the p(n) type. Thus two electrodes of the n^+ type will make possible a separate measurement of the electronic contribution to the conductivity, while two electrodes of the p^+ type will make possible a separate measurement of the hole contribution.

When an external voltage $U_{\rm app}$ is applied between electrodes of the n^+ and p^+ types, electrons and holes are injected until the difference of their Fermi levels is equal to it.[6] The electron conductivity of one layer of a doped GaAs superlattice with $d_{\rm n} = d_{\rm p} = 700$ Å and $n_{\rm D} = n_{\rm A} = 10^{18}$ cm^{-3} can vary from zero up to $1.8 \cdot 10^{-6}\ \Omega^{-1}$, while the hole conductivity can vary from $1.8 \cdot 10^{-5}$ to $5.3 \cdot 10^{-6}\ \Omega^{-1}$.[7] This indicates that doped superlattices can be used as bipolar transistors, which, unlike ordinary field transistors, are volume devices.

A very impressive transport phenomenon occurring in doped superlattices is the giant photoresponse, which is a direct consequence of the exceptionally long lifetime of current carriers (2.40)–(2.41). The ratio of the dc photoresponse of one layer of a doped superlattice $\Delta n^{(2)}_{\rm nipi}$ to that of a bulk semiconductor $\Delta n^{(2)}_{\rm bulk}$ [6]

$$\frac{\Delta n^{(2)}_{\rm nipi}}{\Delta n^{(2)}_{\rm bulk}} \approx \frac{\tau^{\rm rad}_{\rm nipi}}{\tau^{\rm rad}_{\rm bulk}} \tag{5.7}$$

and can exceed 10^{12}. In a doped superlattice of the n type with $d_{\rm n} = d_{\rm p} = 1900$ Å the hole conductivity increases under irradiation by light from $9.3 \cdot 10^{-6}$ to $7.8 \cdot 10^{-5}\ \Omega^{-1}$.[7,183]

The changes induced in the conductivity in the plane of the layers of a doped superlattice by a change in the carrier density are similar to the analogous effects occurring in inverse layers. In particular, phenomena such as the dependence of the mobility on the carrier density, the effect of filling of higher minibands on the mobility, and oscillations of the magnetoresistance have been carefully studied in inversion layers (see, for example, the review of Ref. 179).

The conductivity of doped superlattices along the axis of the superlattice is similar to the analogous conductivity of compositional superlattices and is studied in detail in Ref. 6.

The Hall effect in nonuniformly doped superlattices GaAs–$Al_xGa_{1-x}As$ have been studied experimentally[39] and theoretically.[184] The effect of the current-carrier density and the thickness of the buffer layer (an undoped

$Al_xGa_{1-x}As$ layer) on the Hall mobility has also been studied.[184]

5.2. The Shubnikov–de Haas effect

The quantum motion of current carriers in a direction perpendicular to the layers of the semiconductor superlattice gives rise at low temperatures to two-dimensional motion of the carriers. The dependence of the Shubnikov–de Haas oscillations on the orientation of the magnetic field is a direct proof of this.

The Shubnikov–de Haas effect (oscillations of the transverse magnetoresistance) has been observed in nonuniformly doped type I compositional superlattices $GaAs-Al_xGa_{1-x}As$.[38] In magnetic fields up to 10^4 Oe, with the magnetic field oriented parallel to the axis of the superlattice, distinct oscillations of the transverse magnetoresistance, associated with the change in the scattering of electrons accompanying the crossing of Landau levels with the Fermi energy, were observed. The anisotropy of the Shubnikov–de Haas effect (the oscillations did not occur if the magnetic field was oriented perpendicular to the axis of the superlattice) proves the two-dimensionality of the electron gas in such superlattices. The Shubnikov–de Haas effect makes it possible to study the position of the energy levels.

The period of the oscillations and their extremal points for a magnetic field H_z oriented parallel to the axis of the superlattice are determined from the following condition:

$$\hbar\omega_c (j+\gamma) = E_{F,c}, \quad j = 0, 1, 2, \ldots, \qquad (5.8)$$

where

$$\omega_c = \frac{eH_z}{m_c c}, \quad E_{F,c} = \frac{\pi n^{(2)}\hbar^2}{m_c}, \quad 0<\gamma<1. \qquad (5.9)$$

Here ω_c and m_c are the cyclotron frequency and effective mass of the electrons, and $E_{F,c}$ is the Fermi energy of the two-dimensional electron gas with a density $n^{(2)}$ (for the case when one miniband is filled).

The existence of beats in the Shubnikov–de Haas effect indicates that two minibands of the conduction band are filled in the superlattice $GaAs-Al_xGa_{1-x}As$ with layers ~220 Å thick.[38]

The systematic study of the Shubnikov–de Haas effect in the superlattices $GaAs-Al_xGa_{1-x}As$ made possible the determination of the Fermi surface of these superlattices; the Fermi surface is closed (an ellipsoid with the long axis oriented along the axis of the superlattice), if the Fermi energy is located inside the miniband, or open (a cylinder whose axis is oriented parallel to the axis of the superlattice), if the Fermi energy is located in the minigap.[185]

The oscillatory behavior of the transverse magnetoresistance was observed in semimetallic superlattices InAs-GaSb (Fig. 14).[4] These experiments confirmed the coexistence of electrons and holes in the semimetallic state. Two series of oscillations with the same periods, one of which corresponds to electrons and the other corresponds to holes, were observed. These two periods are almost the same, since the holes in GaSb are formed by the overflow of electrons into InAs and a small excess of electrons exists only because of the small residual doping in InAs.

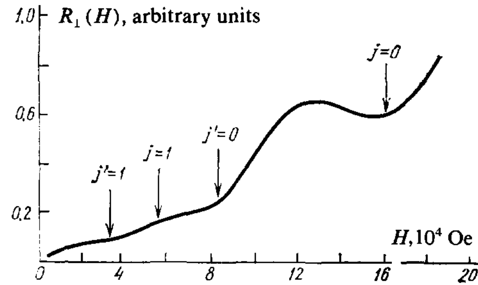

FIG. 14. The dependence of the transverse magnetoresistance $R_\perp(H)$ of the superlattice InAs (120 Å)–GaSb (80 Å) on the magnetic field.[4] $j = 0$ and 1 correspond to extrema on the Fermi surface for $k_z = 0, j' = 0$ and 1 for $k_z = \pm\pi/d$.

The Shubnikov–de Haas effect was also observed in the superlattices InAs-GaSb in the semiconducting state.[4,186] These superlattices were additionally doped in order to achieve a higher electron density.

The dependence of the transverse magnetic resistance on the orientation of the magnetic field indicates the two-dimensionality of the energy minibands in superlattices.

Magnetotransport phenomena have also been studied in the stressed superlattices $GaAs-Ga_{0.8}In_{0.2}As$.[187]

Detailed studies of magnetotransport have confirmed the existence of a quasi-two-dimensional electron system in doped GaAs superlattices. Analysis of the quantum oscillations made possible the determination of the distance between the minibands in the region where the density of excess current carriers is low, which is difficult to study by optical methods[188] (see also the review given in Ref. 189).

Magnetic quantum phenomena in semiconductor superlattices are studied theoretically in Refs. 90, 178, 190–192.

The magnetic susceptibility of semiconductor superlattices is calculated in Ref. 193.

6. THE SEMIMETAL-SEMICONDUCTOR TRANSITION

In this section we shall examine the semimetal-semiconductor transition in superlattices, which has been studied comparatively little experimentally and in great detail theoretically.

In type II compositional superlattices InAs-GaSb (see Fig. 4) the top of the valence band of one semiconductor GaSb ($E_v^{(II)}$) lies above ($\Delta_{vc} \approx 0.15$ eV) the bottom of the conduction band of the other semiconductor InAs ($E_c^{(I)}$). It is therefore energetically advantageous for electrons from the valence band of GaSb to flow into the conduction band of InAs. As a result of this the superlattices will exhibit semimetallic properties. If, however, the superlattice layers are quite thin, then because of size quantization (2.7) the relative arrangement of the lowest minibands of the conduction band of InAs ($E_{c,0}^{(I)}$) and the highest miniband of the valence band of GaSb ($E_{v,0}^{(II)}$) may change, and the superlattice will become a semiconductor (Fig. 5).

To demonstrate experimentally the existence of the semimetal-semiconductor transition, InAs-GaSb superlattices with different periods were grown[4,66,67] and the dependence of the electron density on the thickness of the InAs

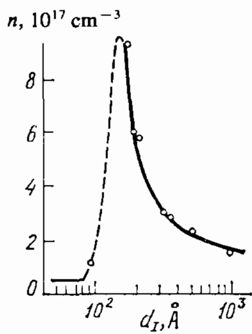

FIG. 15. The dependence of the electron density (n) in the superlattice InAs-GaSb on the thickness of the InAs layer ($d_{\rm I}$), indicating a semimetal (solid line)—semiconductor (broken line) transition.[4]

layers ($d_{\rm I}$) was studied (based on the Hall effect) with $d_{\rm I} = 50$–1000 Å. It turned out that the thickness of the GaSb ($d_{\rm II} = 0.5\, d_{\rm I}$–$d_{\rm I}$) layers had virtually no effect on the electron density.

The electron density decreased sharply when the thickness of the InAs layer became < 100 Å (Fig. 15). The sharp change in the conductivity is not linked with the doping (the impurity concentration $\sim 10^{16}$ cm^{-3}), because the mobility of the electrons $\sim 10^4$ cm^2/v·s at a temperature of 2 K[4] is much higher than in bulk InAs with comparable electron densities.[4,66]

When $d_{\rm I}$ was increased the electron density reached a maximum in the range 100 Å $< d_{\rm I} <$ 200 Å, decreased, and then approached a constant value (see Fig. 15). This is associated with the fact that for large $d_{\rm I}$ the superlattice can be regarded as a system of separate heterocontacts. In this limit electron conduction will occur along the interfaces of the heterocontacts, where the electrons and holes will be concentrated.

The transition from the semimetallic state to the semiconducting state in the superlattices InAs-GaSb was observed not only when $d_{\rm I}$ was decreased, but also when a magnetic field was applied parallel to the axis of the superlattice. This transition occurs in an increasing magnetic field, when the lower Landau level crosses the Fermi level. For InAs-GaSb ($d_{\rm I} = 120$ Å, $d_{\rm II} = 80$ Å and $d_{\rm I} = 200$ Å, $d_{\rm II} = 100$ Å superlattices, which without a magnetic field exhibited semimetallic properties, the transition to the semiconducting state was realized in fields of $1.8 \cdot 10^{15}$ Oe for the first superlattice (see Fig. 14) and $3.46 \cdot 10^5$ Oe for the second superlattice.[4,67]

We indicated above (Sec. 2.1) the complexity of the calculation of the energy structure of type II compositional superlattices. It is interesting to note that the simplest approaches to the calculation of the semimetal-semiconductor transition in these superlattices, such as the semiempirical strong-coupling method (the method of linear combination of atomic orbitals), neglecting the flowing over of current carriers and many-body effects,[41] and the simplest calculations of Eq. (2.8) in Kane's model,[30] give results for the thickness of the layer $d_{\rm I}$ corresponding to the semimetal-semiconductor transition that are in qualitative agreement with the experimental results. The more careful many-band method of envelope functions,[46,47] however, is not in agreement with the experimental results.

In the calculations of the semimetal-semiconductor transition in InAs-GaSb superlattices by the envelope function method,[31,32] the wave functions of the current carriers in each layer are written as a product of a slowly varying envelope function and a Bloch function of the corresponding semiconductors with zero momentum. The envelope functions are solutions of (2.11) in the effective-mass approximation and must satisfy on the interfaces the boundary conditions following from the smoothness of the wave function (see Sec. 2.1).

The calculations[46,47] were performed under the assumption that the effective masses of the current carriers and the Kane matrix elements are the same for both constituent semiconductors of the superlattice. The energy structure of several of the lowest minibands of the conduction band and the upper minibands of the valence band was calculated.

It was shown for $d_{\rm I} = d_{\rm II} = 60$ Å that the superlattice remains a semiconductor (of type III), and the hole minibands are characterized by strong nonparabolicity as a function of $k_\perp$ (in the plane of the superlattice layers).

For $d_{\rm I} = d_{\rm II} = 80$ Å the lowest miniband of the conduction band drops for $k_\perp = 0$, $k_z \neq 0$ below the lowest miniband of the valence band. This intersection is, however, forbidden[46,47] and the system becomes not a semimetal, but rather a zero-gap semiconductor.

For $d_{\rm I} = d_{\rm II} = 90$ Å and $d_{\rm I} = d_{\rm II} = 100$ Å the strong hybridization of the minibands of the valence band and of the conduction band causes the system to become a semiconductor with a very narrow gap of ~ 20 meV.[46,47]

The semiconductor-semimetal transition in such superlattices occurs only for much thicker layers, because of the formation of maxima in the highest filled miniband and minima in the lowest empty miniband with $k_\perp \neq 0$.[46,47]

It should be noted that taking into account the flowing over of current carriers, which destroys electrical neutrality,[194] can substantially change the nature of the semiconductor-semimetal transition.

To eliminate these inconsistencies in the many-band method of envelope functions (see Sec. 2.1) it is necessary to take into account the curvature of the bands, caused by the flowing over of charge, as well as many-body effects, which can be very significant in such strongly anisotropic systems.[52,53] It is also necessary to take into account systematically the motion of current carriers along the interfaces.[29,49] In addition, in order to make an adequate comparison of the theoretical and experimental results the experimental data on the band structure of the constituent semiconductors of the structure (especially Δ_{vc}) must be refined, and it is also necessary to know the values of the effective masses of the holes in thin GaSb layers.[90–92]

Analytic expressions for the effective masses of size-quantized holes in semiconductors with a degenerate valence band are available only for infinitely deep potential wells with $k_\perp d_{\rm II} \ll \sqrt{\pi(j+1)}$:

$$\frac{1}{m_{lh,\,j}} = \frac{1}{m_{lh}} \left\{ 1 + \frac{3\sqrt{\tilde\beta}}{\pi(j+1)} \; \frac{(-1)^j + \cos[\pi(j+1)/\beta^{1/2}]}{\sin[\pi(j+1)/\beta^{1/2}]} \right\}, \tag{6.1}$$

$$\frac{1}{m_{\mathrm{hh},j}}=\frac{1}{m_{\mathrm{hh}}}\left\{1+\frac{3}{\pi\sqrt{\beta}\,(j+1)}\,\frac{(-1)^{j}+\cos[\pi(j+1)\beta^{1/2}]}{\sin[\pi(j+1)\beta^{1/2}]}\right\}, \tag{6.2}$$

where $m_{\mathrm{hh(lh)}}$ is the effective mass of heavy (light) holes in the bulk semiconductor and $\beta = m_{\mathrm{lh}}/m_{\mathrm{hh}}$, $j = 0, 1, 2,...$ is the number of the hole miniband[200,201]; for potential wells of finite depth (a double heterojunction (see Fig. 1) $Al_{0.24}Ga_{0.76}As$–GaAs–$Al_{0.24}Ga_{0.76}As$[192]) only numerical calculations have been performed. These calculations[192,200,201] indicate a substantial nonparabolicity of the dependence of the energy size-quantized holes on the quasi-momentum perpendicular to the axis of the superlattice (in particular, the dispersion of some hole subbands will have an electronic character).

The semiconductor—zero-gap-semiconductor transition can occur in HgTe-CdTe superlattices.[32]

The transition from the semiconductor to the semimetal states can also occur in doped superlattices. When the impurity concentration or the period of the superlattice is increased, the amplitude of the superlattice potential $2V_0$ (2.27) can exceed the energy gap of the starting semiconductor E_g^0 (Fig. 16). In this case the electrons and holes occupy the bottom minibands of the conduction band and the top minibands of the valence band, respectively, forming a quasi-two-dimensional electron-hole system in the ground state. The doped GaAs superlattice becomes semimetallic at $n_D = n_A = 10^{18}$ cm^{-3} if $d_n = d_p > 700$ Å.[6]

In most cases the electron-hole system in semiconductor superlattices can be regarded as two-dimensional, though the quite large width of the minibands (~ 20 meV) for the type II superlattice InAs-GaSb with layers ~ 100 Å thick indicates the three-dimensionality of the band structure.[195] The transition from two- to three-dimensional motion of the current carriers, which is manifested as a substantial broadening of the electronic minibands, was observed in doped superlattices GaAs ($d_n = d_p = 400$ Å, $n_D = n_A = 10^{18}$ cm^{-3} when the intensity of the optical excitation was increased. This is also indicated by the fact that when the intensity is increased interminiband transitions in these superlattices coalesce into a wide band of single-particle excitations.[142,196]

7. CONCLUSIONS

Superlattices provide a unique possibility for changing their band structure in a practically arbitrary manner (band engineering). This makes it possible, in particular, to change substantially their transport properties, creating low-noise avalanche detectors, photomultipliers, ultrafast devices, photodetectors, and other devices based on superlattices.[197,198]

Superlattices exhibit the interesting property that the form of the potential in them can be changed practically arbitrarily, i.e., the wave function of the current carriers can be changed in a controllable fashion (wave-function engineering).[199]

The characteristic features of the luminescence of type I compositional superlattices (variation of the emitted wavelengths with the width of the quantum well, the exciton character of the radiation up to room temperatures, much higher suppression of impurity trapping than in bulk semiconductors of the same quality, simpler fabrication technology of light-emitting devices than for quaternary compounds, femtosecond kinetics, possibility of obtaining large as well as differential amplifications, high injection efficiency (and therefore high device efficiency also), can be (and are) exploited to create a new generation of light-emitting devices.[11] The class of semiconductors used for making superlattices is rapidly expanding. Thus superlattices consisting of group IV semiconductors have recently been synthesized: Ge-$Ge_{1-x}Si_x$[202] and Si-$Si_{1-x}Ge_x$.[203] Superlattices consisting of semiconductors and dielectrics could have interesting properties: Ge-BaF_2 and InP-BaF_2.[204]

The study of semiconductor superlattices is now progressing rapidly. This is reflected in the avalanche-like increase in the number of publications. Thus if only the theoretical and experimental papers on superlattices synthesized from A_3B_5 compounds by the method of molecular-beam epitaxy are counted, then 39 publications appeared in 1980, 59 in 1981, 97 in 1982, and 143 in 1983.[20]

In spite of the rapid growth in the number of both theoretical and experimental studies devoted to semiconductor superlattices, many problems still await a solution.

The systematic calculation of minibands of a compositional superlattice can only be carried out at the present time in the case when the masses of the electrons (holes) are the same in both constituent semiconductors of the superlattice, because only in this case is it possible to separate the motion of current carriers along and perpendicular to the axis of the superlattice.[29,49]

It is undoubtedly of interest to study the collective properties of the current carriers in semiconductor superlattices.

In conclusion I want to thank L. V. Keldysh for numerous discussions and valuable remarks and V. S. Bagaev for his stimulating interest in this work.

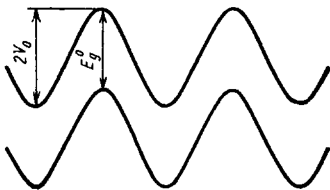

FIG. 16. Semimetallic doped superlattice.

1. L. V. Keldysh, Fiz. Tverd. Tela **4**, 2265 (1962) [Sov. Phys. Solid State **4**, 1658 (1963)].
2. L. L. Chang, L. Esaki, W. E. Howard, R. Ludeke, and G. Schul, J. Vac. Sci. Technol. **10**, 655 (1973).
3. A. Y. Cho and J. R. Arthur, Progr. Sol. State Chem. **10**, 157 (1975).
4. L. Esaki, Lect. Not. Phys. **133**, 302 (1980).
5. G. H. Dohler and K. Ploog, Progr. Cryst. Growth Charact. **2**, 145 (1979).
6. K. Ploog and G. H. Dohler, Adv. Phys. **32**, 285 (1983).
7. K. Ploog, Spring Ser. Sol. State Sci. **53**, 220 (1984).

[8]G. Weimann and W. Schlapp, *ibid.*, 88.
[9]M. Razeghi and J. P. Duchemin, *ibid.*, 100.
[10]S. V. Gaponov, B. M. Luskin, and N. N. Salashchenko, Pis'ma Zh. Tekh. Fiz. **5**, 516 (1979) [Sov. Phys. Tech. Phys. **5**, 210 (1979)].
[11]H. Clemens, E. J. Fahter, and G. Cauer, Rev. Sci. Instr. **54**, 685 (1983).
[12]G. H. Dohler, Phys. Scripta **24**, 230 (1981).
[13]L. Esaki and R. Tsu, IBM J. Res. Develop. **14**, 61 (1970).
[14]R. J. Stiles, Surf. Sci. **73**, 451 (1978).
[15]V. A. Volkov, V. A. Petrov, and V. B. Sandomirskiĭ, Usp. Fiz. Nauk **131**, 423 (1980) [Sov. Phys. Usp. **23**, 375 (1980)].
[16]M. von Ortenberg, Phys. Rev. Lett. **49**, 1041 (1982).
[17]L. A. Kolodzievski, T. C. Bonsett, R. L. Bunshor, S. Datta, R. B. Bylsma, W. M. Becker, and N. Otsuka, Appl. Phys. Lett. **45**, 440 (1984).
[18]A. A. Kastal'skiĭ, Pis'ma Zh. Eksp. Teor. Fiz. **10**, 328 (1969) [JETP Lett. **10**, 209 (1969)].
[19]A. Ya. Shik, Fiz. Tekh. Poluprovodn. **8**, 1841 (1974) [Sov. Phys. Semicond. **8**, 1195 (1974)].
[20]K. Ploog and K. Graf, Molecular Beam Epitaxy of III-V Compounds, Springer-Verlag, Berlin (1984).
[21]L. Esaki in: Proceedings of International Conference on Physics of Heterojunctions, Budapest (1971), Vol. 1, p. 383.
[22]Zh. I. Alferov, Yu. V. Zhilyaev, and Yu. V. Shmartsev, Fiz. Tekh. Poluprovodn. **5**, 196 (1971) [Sov. Phys. Semicond. **5**, 174 (1971)].
[23]M. Grimsditch, M. R. Khan, A. Kueng, and I. K. Schuller, Phys. Rev. Lett. **51**, 498 (1983).
[24]I. Banerjee and I. K. Schuller, J. Low Temp. Phys. **54**, 506 (1984).
[25]G. J. Iafrate, D. K. Ferry, and R. K. Reich, Surf. Sci. **113**, 485 (1982).
[26]R. K. Reich, D. K. Ferry, and R. O. Crondin, Phys. Rev. B **27**, 3483 (1983).
[27]A. A. Ignatov, Dokl. Akad. Nauk SSSR **273**, 1351 (1893) [Sov. Phys. Dokl. **28**, 1046 (1983)].
[28]N. N. Meiman, J. Math. Phys. **24**, 539 (1983).
[29]D. Mukherji and B. R. Nag, Phys. Rev. B **30**, 651 (1975).
[30]B. A. Sai-Halasz, R. Tsu, and L. Esaki, Appl. Phys. Lett. **30**, 651 (1977).
[31]G. Bastard, Phys. Rev. B **24**, 5693 (1981).
[32]G. Bastard, *ibid.* **25**, 7584.
[33]G. Bastard, Springer Ser. Sol. State Sci. **53**, 168 (1984).
[34]E. O. Kane, J. Phys. Chem. Sol. **1**, 249 (1957).
[35]Y. Goldner, Springer Ser. Sol. State Sci. **53**, 200 (1984).
[36]W. Andreoni and A. Baldereschi, Solid State Commun. **27**, 821 (1978).
[37]A. Madhukar and J. Delgado, *ibid.* **37**, 199 (1981).
[38]T. Dingle, H. L. Stormer, A. C. Gossard, and W. Wiegmann, Appl. Phys. Lett. **33**, 665 (1978).
[39]H. L. Stormer, A. Pinczuk, A. C. Gossard, and W. Wiegmann, *ibid.* **38**, 691 (1981).
[40]T. J. Drummond, J. Klein, D. Arnold, R. Fisher, R. E. Thorne, W. G. Lyons, and H. Markoc, *ibid.* **42**, 615 (1983).
[41]G. A. Sai-Halasz, L. Esaki, and W. Harrison, Phys. Rev. B **18**, 2812 (1978).
[42]J. Ihm, P. K. Lam, and M. L. Cohen, *ibid.* **20**, 4120 (1979).
[43]S. R. White and L. J. Shame, Phys. Rev. Lett. **47**, 879 (1981).
[44]S. R. White and L. J. Shame, Surf. Sci. **113**, 131 (1982).
[45]L. L. Chang, N. J. Kawai, E. E. Mendez, C.-A. Chang, and L. Esaki, Appl. Phys. Lett. **38**, 30 (1981).
[46]M. Altarelli, Lect. Not. Phys. **177**, 174 (1983).
[47]M. Altarelli, Phys. Rev. B **28**, 842 (1983).
[48]A. D. Madhukar, N. V. Dandekar, and R. N. Nucho, J. Vac. Sci. Technol. **16**, 1507 (1979).
[49]M. de Dios Leyva, R. P. Alvarez, and J. L. Gondar, Phys. Status Solidi B **125**, 221 (1984).
[50]H. Takaoka, C.-A. Chang, E. E. Mendez, L. L. Chang, and L. Esaki, Physica B **117-118**, 741 (1983).
[51]P. Voisin, Springer Ser. Sol. State Sci. **53**, 192 (1984).
[52]E. A. Andryushin, V. S. Babichenko, O. V. Keldysh, T. A. Onishchenko, and A. P. Silin, Pis'ma Zh. Eksp. Teor. Fiz. **24**, 210 (1976) [JETP Lett. **24**, 185 (1976)].
[53]E. A. Andryushin and A. P. Silin, Fiz. Tverd. Tela **19**, 1405 (1977) [Sov. Phys. Solid State **19**, 815 (1977)].
[54]M. J. Ludowise, W. T. Dietze, C. R. Lewis, N. Holonyak Jr., K. Hess, M. D. Camras, and M. A. Nixon, Appl. Phys. Lett. **42**, 257 (1983).
[55]M. D. Camras, J. M. Brown, N. Holonyak Jr., M. A. Nixon, R. W. Kalinsky, M. J. Ludowise, W. T. Dietze, and C. R. Lewis, J. Appl. Phys. **54**, 6183 (1983).
[56]I. J. Frietz, R. M. Biefeld, and G. C. Osbourn, Solid State Commun. **45**, 323 (1983).
[57]P. L. Gourley and R. M. Beifeld, J. Vac. Sci. Technol. B **1**, 383 (1983).
[58]S. T. Picraux, L. R. Dawson, G. C. Osbourn, and W. K. Chu, Appl. Phys. Lett. **43**, 930 (1983).
[59]I. J. Fritz, L. R. Dawson, and T. E. Zipperian, J. Vac. Sci. Technol. B **1**, 387 (1983).
[60]J. Y. Marzin and E. V. K. Rao, Appl. Phys. Lett. **43**, 560 (1983).
[61]D. L. Smith, T. C. McGill, and J. N. Schulman, *ibid.*, 180.
[62]C. -A. Chang, H. Takaoka, L. L. Chang, and L. Esaki, *ibid.* **40**, 983 (1982).
[63]P. Voisin, E. Bastard, M. Voos, E. E. Mendez, L. L. Chang, and L. Esaki, J. Vac. Sci. Technol. B **1**, 152 (1983).
[64]G. Griffiths, K. Mohammed, S. Subbana, H. Kroemer, and J. Merz, Appl. Phys. Lett. **43**, 1059 (1983).
[65]E. E. Mendez, C.-A. Chang, H. Takaoka, L. L. Chang, and L. Esaki, J. Vac. Sci. Technol. B **1**, 152 (1983).
[66]L. L. Chang, N. Kawai, G. A. Sai-Halasz, R. Ludeke, and L. Esaki, Appl. Phys. Lett. **35**, 939 (1979).
[67]L. L. Chang, J. Phys. Soc. Jpn. Suppl. A **49**, 997 (1980).
[68]Y. Guldner, Physica B **117-118**, 735 (1983).
[69]H. Fujiyasu, H. Takahashi, H. Shimizu, A. Sasaki, and H. Kuwabara, Proceedings of the 17th International Conference of Physics Semiconductors, San Francisco, 1984, Springer-Verlag, New York (1984), p. 539.
[70]F. Capasso, S. Luryi, W. T. Tsang, C. G. Bethea, and B. F. Levine, Phys. Rev. Lett. **51**, 2318 (1983).
[71]A. N. Lobaev and A. P. Silin, Kr. soobshch. fiz. (FIAN SSSR), No. 1, 19 (1985).
[72]B. Abeles and T. Tiedje, Phys. Rev. Lett. **51**, 2003 (1983).
[73]T. Tiedje and B. Abeles, Appl. Phys. Lett. **45**, 179 (1984).
[74]T. Ogino and Y. Mizushima, Jpn. J. Appl. Phys. **22**, 1647 (1983).
[75]V. S. Gaponov, V. M. Luskii, and N. N. Salashchenko, Pis'ma Zh. Eksp. Teor. Fiz. **33**, 533 (1981) [JETP Lett. **33**, 517 (1981)].
[76]A. Sasaki, Phys. Rev. B **30**, 7016 (1984).
[77]Yu. A. Romanov, Fiz. Tekh. Poluprovodn. **5**, 1431 (1971) [*sic*]. V. I. Stafeev, *ibid.*, 408 [*ibid.* 359]. G. H. Dohler Phys. Status Solidi B **52**, 533 (1972); **53**, 79.
[78]P. Ruden and G. H. Dohler, Phys. Rev. B **27**, 3538 (1983).
[79]H. Kunzel, A. Fisher, J. Knecht, and K. Ploog, Appl. Phys. A **30**, 73 (1983).
[80]G. H. Dohler in: Proceedings of the 17th International Conference of Physics Semiconductors, San Francisco, 1984, Springer-Verlag, New York (1984), p. 491.
[81]M. Hundhausen, J. Wagner, and L. Ley, *ibid.*, p. 495.
[82]J. Kakalios and H. Frietzsche, *ibid.*, p.503.
[83]J. C. Maan, Springer Ser. Sol. State Sci. **53**, 183 (1984).
[84]F. Stern, Phys. Rev. Lett. **18**, 546 (1967).
[85]E. A. Andryushin and A. P. Silin, Fiz. Tverd. Tela **18**, 2130 (1976) [Sov. Phys. Solid State **18**, 1243 (1976)].
[86]G. M. Shmelev, I. A. Chaikovskii, V. V. Pavlovich, and E. M. Epstein, Phys. Status Solidi B **82**, 391 (1977).
[87]W. L. Bloss, Solid State Commun. **44**, 363 (1982).
[88]D. Olego, A. Pinczuk, A. C. Gossard, and W. Wiegmann, Phys. Rev. B **25**, 7867 (1982).
[89]A. C. Thelis, G. Gonzalez de la Crus, and J. J. Quinn, Solid State Commun. **47**, 43 (1983).
[90]J. C. Maan, M. Altarelli, H. Sigg, P. Wyder, L. L. Chang, and L. Esaki, Surf. Sci. **113**, 347 (1982).
[91]G. F. Giuliani and J. J. Quinn, Phys. Rev. Lett. **51**, 919 (1983).
[92]G. Qin, G. F. Giuliani, and J. J. Quinn, Phys. Rev. B **28**, 6144 (1983).
[93]S. Datta and R. L. Gunsher, J. Appl. Phys. **28**, 6144 (1983).
[94]A. C. Tselis and J. J. Quinn, Phys. Rev. B **29**, 3318 (1984).
[95]G. Bastard, E. E. Mendez, L. L. Chang, and L. Esaki, Phys. Rev. B **26**, 1974 (1982).
[96]R. L. Greene and K. K. Bajaj, Solid State Commun. **45**, 831 (1983).
[97]R. R. Guseinov, Phys. Status Solidi B **125**, 237 (1984).
[98]E. A. Andryushin and A. P. Silin, Fiz. Tverd. Tela **22**, 2676 (1980) [Sov. Phys. Solid State **22**, 1562 (1980)].
[99]Yu. E. Lozovik and V. N. Nishanov, Fiz. Tverd. Tela **18**, 3267 (1976) [Sov. Phys. Solid State **18**, 1905 (1976)].
[100]F. Crowne, T. L. Reinecke, and B. V. Shanabrook in: Proceedings of the 17th International Conference of Physics Semiconductors, San Francisco, 1984, Springer-Verlag, New York (1984), p. 363.
[101]Y. Goldner, J. P. Vieren, M. Voos, L. L. Chang, and L. Esaki, Phys. Rev. Lett. **45**, 1719 (1980).
[102]Y. Guldner, J. P. Keren, P. Voisin, M. Voos, J. C. Maan, L. L. Chang, and L. Esaki, Solid State Commun. **41**, 755 (1982).
[103]E. J. Fanter and G. Bauer, Springer Ser. Sol. State Sci. **53**, 207 (1984).

[104]L. C. Chin, J. C. Smith, S. Margalit, and A. Yariv, Appl. Phys. Lett. **43**, 331 (1983).
[105]H. Adamska and H. N. Spector, J. Appl. Phys. **56**, 1123 (1984).
[106]R. Dingle, W. Wiegmann, and C. H. Henry, Phys. Rev. Lett. **33**, 827 (1974).
[107]R. Dingle, A. C. Gossard, and W. Wiegmann, *ibid.* **34**, 1327 (1975).
[108]R. C. Miller, D. A. Kleinmann, W. T. Tsang, and A. S. Gossard, Phys. Rev. B **24**, 1134 (1981).
[109]D. A. B. Miller, D. S. Chemla, D. J. Eilenberger, P. W. Smith, A. C. Gossard, and W. T. Tsang, Appl. Phys. Lett. **41**, 679 (1982).
[110]H. M. Gibbs, S. S. Tarug, J. L. Jewell, D. A. Weinberger, K. Tai, A. C. Coscard, S. L. McCall, A. Passner, and W. Wiegmann, *ibid.*, 221.
[111]D. Bimberg, J. Christen, and A. Steckenborn, Springer Ser. Sol. State Sci. **53**, 136 (1984).
[112]Z. Y. Xu, V. G. Kreimanis, and C. L. Tang, Appl. Phys. Lett. **43**, 415 (1983).
[113]C. Weisbuch, R. C. Miller, R. Dingler, A. C. Gossard, and W. Wiegmann, Solid State Commun. **37**, 219 (1981).
[114]B. Lamberg, B. Deveand, A. Regreny, and G. Talalaeff, Physica B **117–118**, 717 (1983).
[115]G. Bastard, Phys. Rev. B **24**, 4714 (1981).
[116]N. C. Jarosik, B. D. McCombe, B. V. Shanabrook, J. Comas, and G. Wicks in: Proc. Seventeenth Intern. Conf. of Physics Semiconductors, San Francisco, 1984, Springer-Verlag, New York, 1984, p. 507.
[117]C. Mailhot, Y. C. Chang, and T. C. McGill, Phys. Rev. B **26**, 4449 (1982).
[118]a) G. Bastard, C. Delande, M. H. Meynadier, P. M. Frijlink, and M. Voos, *ibid.* **29**, 7042 (1984). b) D. A. Kleinmann, *ibid.* **28**, 871 (1983).
[119]D. S. Chemla, T. C. Damen, D. A. B. Miller, A. C. Gossard, and W. Wiegmann, Appl. Phys. Lett. **42**, 864 (1983).
[120]D. A. B. Miller, D. S. Chemla, T. C. Damen, A. C. Gossard, W. Wiegmann, T. H. Wood, and C. A. Burrus, Phys. Rev. Lett. **54**, 2173 (1984).
[121]R. C. Miller and A. C. Gossard, Appl. Phys. Lett. **43**, 954 (1983).
[122]N. Miura, Y. Iwasa, S. Tarucha, and H. Okamoto in: Proc. Seventeenth Intern. Conf. on Physics of Semiconductors, San Francisco, 1984, Springer-Verlag, New York (1984), p. 359.
[123]J. C. Maan, A. Fasolino, G. Belle, M. Altarelli, and K. Ploog, *ibid.*, p. 463.
[124]Y. Aoyagi, Y. Segawe, T. Miyoshi, and S. Namba, *ibid.*, p. 571.
[125]a) I. A. Chaikovskii, G. M. Shmelev, and N. A. Enaki, Phys. Status Solidi B **108**, 732 (1981). b) H. Q. Le, B. Lax, B. A. Vojak, A. R. Calava, and W. D. Goodhye in: Proc. Seventeenth Intern. Conf. on Physics of Semiconductors, San Francisco, 1984, Springer-Verlag, New York (1984), p. 515.
[126]a) E. A. Andryushin and A. P. Silin, Fiz. Nizk. Temp. **3**, 1365 (1977) [Sov. J. Low Temp. Phys. **3**, 655 (1977)]. b) P. Dawson, G. Duggan, H. J. Ralph, and K. W. Woodbridge, *ibid.*, p. 551 [*sic*].
[127]J. E. Fouquet, A. E. Siegman, and A. C. Gossard, *ibid.*, p. 583 [*sic*].
[128]Y. Mesumoto, S. Shionoya, and H. Okamoto, *ibid.*, p. 349 [*sic*].
[129]a) N. Peyghambarian, H. M. Gibbs, J. L. Jewell, A. Antonetti, A. Migus, D. Hulin, and A. Mysorowics, Phys. Rev. Lett. **29**, 7065 (1984). b) J. E. Zucker, A. Pinczuk, D. S. Chemla, A. Gossard, and W. Wiegmann, Phys. Rev. B **29**, 7065 (1984).
[130]N. Holonyak Jr., R. M. Kolbas, W. D. Laidig, B. A. Vojak, R. D. Dupuis, and P. D. Dapkus, Appl. Phys. Lett. **33**, 737 (1978).
[131]H. Kawai, O. Matsuda, and K. Kaneko, Jpn. J. Appl. Phys. **22**, L727 (1983).
[132]H. Iwamura, S. Sarucha, T. Sanu, Y. Horikoshi, and H. Okamoto, *ibid.*, L751.
[133]W. T. Tsang, Appl. Phys. Lett. **39**, 786 (1981).
[134]R. Chiu, N. Holonjak Jr., B. A. Vojak, K. Hess, R. D. Dupuis, and P. D. Dapkus, *ibid.* **36**, 19 (1980).
[135]N. K. Datta, J. Appl. Phys. **54**, 1236 (1983).
[136]G. A. Sai-Halasz, L. L. Chang, J.-M. Welter, C.-A. Chang, and L. Esaki, Solid State Commun. **26**, 935 (1978).
[137]K. Ploog and H. Kunzel, Microelectron. J. **13**, 111 (1982).
[138]L. V. Keldysh, Zh. Eksp. Teor. Fiz. **34**, 1138 (1958) [Sov. Phys. JETP **7**, 788 (1958)], W. Franz, Z. Naturforsch. A **13**, 484 (1958).
[139]G. H. Dohler, H. Kunzel, and K. Ploog, Phys. Rev. B. **25**, 2618 (1982).
[140]P. P. Ruden and G. H. Dohler in: Proc. Seventeenth Intern. Conf. on Physics of Semiconductors, San Francisco, 1984, Springer-Verlag, New York (1984), p. 535.
[141]H. Jung, H. Kunzel, G. H. Dohler, and K. Ploog, J. Appl. Phys. **54**, 6965 (1983).
[142]Ch. Zeller, B. Vinter, G. Abstreiter, and K. Ploog, Phys. Rev. B **26**, 2124 (1982).
[143]G. H. Dohler, H. Kunzel, D. Olego, K. Ploog, P. Ruden, H. J. Stolz, and G. Abstreiter, Phys. Rev. Lett. **47**, 864 (1981).
[144]H. Jung, G. H. Dohler, H. Kunzel, K. Ploog, P. Ruden, and H. J. Stolz, Solid State Commun. **43**, 291 (1982).
[145]H. Kunzel, G. H. Dohler, P. Ruden, and K. Ploog, Appl. Phys. Lett. **41**, 852 (1982).
[146]W. Rehm, H. Kunzel, G. H. Dohler, K. Ploog, and P. Ruden, Physica B **117-118**, 732 (1983).
[147]G. Abstreiter, Springer Ser. Sol. State Sci. **53**, 232 (1984).
[148]V. Narayanamurti, H. L. Stormer, M. A. Shin, A. C. Gossard, and W. Wiegmann, Phys. Rev. Lett. **43**, 2012 (1979).
[149]C. Colvard, R. Merlin, M. V. Klein, and A. C. Gossard, *ibid.* **45**, 298.
[150]B. Jusserand, D. Paquet, A. Regreny, and J. Kervaree, Solid State Commun. **48**, 499 (1983).
[151]K. Kubota, N. Nakajima, H. Katoh, and N. Sano, *ibid.* **49**, 157 (1984).
[152]J. J. Quinn, V. Strom, and L. L. Chang, *ibid.* **45**, 111 (1983).
[153]R. J. Nicholas, M. A. Brummell, and J. C. Portal, Springer Ser. Sol. State Sci. **53**, 69 (1984).
[154]G. M. Schmelev, I. A. Chaikovskii, V. V. Pavlovich, and E. M. Epstein, Phys. Status Solidi B **80**, 697 (1977).
[155]E. P. Pokatilov and S. J. Beril, *ibid.* **110**, K75 (1982).
[156]E. P. Pokatilov and S. J. Beril, *ibid.* **118**, 567 (1983).
[157]S. V. Kryuohkov, Fiz. Tverd. Tela **20**, 2795 (1978) [Sov. Phys. Solid State **20**, 1612 (1978)].
[158]E. M. Epshtein, Fiz. Tekh. Poluprovodn. **13**, 611 (1979) [Sov. Phys. Semicond. **13**, 360 (1979)].
[159]G. M. Shmelev, Shon Nguen Hong, and G. I. Tsurkan, J. Phys. C **16**, 2587 (1983).
[160]G. M. Shmelev, Shon Nguen Hong, and Anhy Vo Hung, Solid State Commun. **48**, 239 (1983).
[161]R. J. Nicholas, Contemp. Phys. **21**, 501 (1980).
[162]R. Tsu and L. Esaki, Appl. Phys. Lett. **19**, 246 (1971).
[163]L. V. Keldysh, Zh. Eksp. Teor. Fiz. **43**, 661 (1962) [Sov. Phys. JETP **16**, 471 (1963)].
[164]A. A. Ignatov and Yu. A. Romanov, Phys. Status Solidi B **73**, 327 (1976).
[165]A. A. Ignatov, Izv. Vyssh. Uchebn. Zaved., Radiofiz. **25**, 1547 (1982).
[166]S. A. Ktitorov, G. S. Simin, and V. Ya. Sindalovskii, Fiz. Tverd. Tela **13**, 2230 (1971) [Sov. Phys. Solid State **13**, 1872 (1971)].
[167]F. G. Bass and E. A. Rubinshtein, Fiz. Tverd, Tela **19**, 1379 (1977) [Sov. Phys. Solid State **19**, 800 (1977)].
[168]A. A. Ignatov and Yu. A. Romanov, Fiz. Tverd. Tela **17**, 3388 (1975) [Sov. Phys. Solid State **17**, 2216 (1975)].
[169]V. V. Pavlovich and E. M. Epshtein, Fiz. Tverd. Tela **18**, 1483 (1976) [Sov. Phys. Solid State **18**, 863 (1976)].
[170]A. A. Ignatov and Yu. A. Romanov, Izv. Vyssh. Uchebn. Zaved., Radiofiz. **21**, 132 (1978).
[171]A. A. Ignatov and V. I. Shashkin, Phys. Status Solidi B **110**, K117 (1982).
[172]A. A. Ignatov and V. I. Shashkin, Phys. Lett. A **94**, 169 (1983).
[173]S. V. Kryuchkov and M. V. Vyazovskii, Fiz. Tverd. Tela **21**, 3182 (1979) [Sov. Phys. Solid State **21**, 1836 (1979)].
[174]A. A. Ignatov, Fiz. Tverd. Tela **22**, 3319 (1980) [Sov. Phys. Solid State **22**, 1942 (1980)].
[175]R. F. Kazarinov and R. A. Suris, Fiz. Tekh. Poluprovodn. **6**, 148 (1972) [Sov. Phys. Semicond. **6**, 120 (1972)].
[176]G. M. Shmelev, I. A. Chaikovskii, and Shon Chan Min, Phys. Status Solidi B **76**, 811 (1976).
[177]G. M. Shmelev, I. A. Chaikovskii, and Bau Nguen Kuang, Fiz. Tekh. Poluprovodn. **12**, 1932 (1978) [Sov. Phys. Semicond. **12**, 1149 (1978)].
[178]V. M. Polyanovskiĭ, Fiz. Tverd. Tela **22**, 1975 (1980) [Sov. Phys. Solid State **22**, 1151 (1980)].
[179]T. Ando, A. B. Fowler, and F. Stern, Rev. Mod. Phys. **43**, 437 (1982).
[180]L. Esaki and L. L. Chang, Phys. Rev. Lett. **33**, 495 (1974).
[181]R. Tsu, L. L. Chang, G. A. Sai-Halasz, and L. Esaki, *ibid.* **34**, 1509 (1975).
[182]K. Hess, Physica B **117-118**, 723 (1983).
[183]H. Kunzel, G. H. Dohler, and K. Ploog, Appl. Phys. A **27**, 1 (1982).
[184]G. Fishman and D. Caleski, Phys. Rev. B **29**, 5778 (1984).
[185]J. Yoshino, H. Sakaki, and T. Furita in: Proc. Seventeenth Intern. Conf. on Physics of Semiconductors, San Francisco, 1984, Springer-Verlag, New York (1984), p. 519.
[186]H. Sakaki, L. L. Chang, G. A. Sai-Halasz, C.-A. Chang, and L. Esaki, Solid State Commun. **26**, 589 (1978).
[187]J. E. Schrieber, I. J. Frietz, L. R. Dawson, and G. C. Osbourn, Phys. Rev. B **28**, 2229 (1983).
[188]J. C. Maan, T. Anglert, C. Vihlein, H. Kunzel, K. Ploog, and A. Fisher,

J. Vac. Sci. Technol. B **1**, 289 (1983).
[189]J. C. Maan, Springer Ser. Sol. State Sci. **53**, 183 (1984).
[190]R. Tsu and J. Janak, Phys. Rev. B **9**, 404 (1974).
[191]I. A. Chaikovskii, G. M. Shmelev, and Chang Quang Hung, J. Phys. C **10**, 3315 (1977).
[192]A. Fasolino and M. Altarelli, Springer Ser. Sol. State Sci. **53**, 176 (1984).
[193]S. K. Lyo, Solid State Commun. **51**, 709 (1984).
[194]E. A. Andryushin and A. P. Silin, Fiz. Tverd. Tela **23**, 3399 (1981) [Sov. Phys. Solid State **23**, 1972 (1981)].
[195]J. C. Maan, Y. Guldner, J. D. Vieren, P. Voisin, M. Voos, L. L. Chang, and L. Esaki, Surf. Sci. **113**, 313 (1983).
[196]Ch. Zeller, B. Vinter, G. Abstreiter, and K. Ploog, Physica B **117-118**, 719 (1983).
[197]F. Capasso, J. Vac. Sci. Technol. B **1**, 457 (1983); Physica B **129**, 92 (1985).
[198]F. Capasso in: Proc. Seventeenth Intern. Conf. on Physics of Semiconductors, San Francisco, 1984, Springer-Verlag, New York (1984), p. 1537.
[199]H. Sakaki, *ibid.*, p. 1551.
[200]S. S. Nedorezov, Fiz. Tverd, Tela **12**, 2270 (1970) [*sic*].
[201]M. I. D'yakonov and A. V. Khaetskiĭ, Zh. Eksp. Teor. Fiz. **82**, 1584 (1982) [Sov. Phys. JETP **55**, 917 (1982)].
[202]A. M. Belyantsev, E. A. Erofeev, A. A. Ignatov, O. A. Kuznetsov, V. I. Piskarev, Yu. A. Romanov, V. A. Tolmasov, and V. I. Shashkin, Preprint No. 101, Institute of Applied Physics of the USSR Academy of Sciences, Gor'kiĭ (1984).
[203]J. C. Bean, L. C. Feldman, A. T. Fiory, S. Nakahara, and I. K. Robinson, J. Vac. Sci. Technol. A **2**, 436 (1984).
[204]V. Narayanamurti, Phys. Today **37**, 24 (1984).

Translated by M. E. Alferieff